Electroweak corrections to Z-boson hadroproduction at finite transverse momentum

W. Hollik,[a] B. A. Kniehl,[b] E. S. Scherbakova,[b] O. L. Veretin[b]

a Max-Planck-Institut für Physik (Werner-Heisenberg-Institut),

Föhringer Ring 6, 80805 München, Germany

b II. Institut für Theoretische Physik, Universität Hamburg,

Luruper Chaussee 149, 22761 Hamburg, Germany

Abstract

We calculate the full one-loop electroweak radiative corrections, of $\mathcal{O}(\alpha^2\alpha_s)$, to the cross section of single Z-boson inclusive hadroproduction at finite transverse momentum (p_T). This includes the $\mathcal{O}(\alpha)$ corrections to $Z + j$ production, the $\mathcal{O}(\alpha_s)$ corrections to $Z + \gamma$ production, and certain QCD-electroweak interference contributions involving a single quark trace. We recover the QCD and purely weak corrections and study the QED corrections and the QCD-electroweak interference contributions for the first time. We also consider direct and resolved photoproduction in elastic and inelastic scattering. We present p_T and rapidity distributions for the experimental conditions at the Fermilab Tevatron and the CERN LHC and assess the significance of the various contributions.

PACS numbers: 12.15.Lk, 12.38.Bx, 13.85.Qk, 14.70.Hp

1   Introduction

The study of single electroweak-gauge-boson hadroproduction, via the so-called Drell–Yan process, has a long history, starting from the discovery of the W [1] and Z [2] bosons at the CERN Super Proton Synchrotron (SPS) more than three decades ago, which marked a breakthrough for the Standard Model (SM). These processes remain to be of paramount importance also at modern hadron colliders, such as the Fermilab Tevatron and the CERN LHC. On the one hand, they have large cross sections and clean decay signatures in the detectors. This renders them particularly useful for calibrating and monitoring the luminosities at hadron colliders, which affects all other cross section measurements performed there as well. By the same token, they are sensitive probes of the parton density functions (PDFs), in partiular of those of the quarks and antiquarks. On the other hand, singly produced W and Z bosons form important backgrounds for searches of new physics beyond the SM, such as anomalous couplings, extra vector bosons, etc.

To achieve an adequate theoretical description, radiative corrections, both of QCD and electroweak type, must be taken into account. As for the total cross sections of single W- and Z-boson hadroproduction, the next-to-leading-order (NLO) [3] and next-to-next-to-leading-order (NNLO) [4] QCD corrections were calculated a long time ago, and also partial results at next-to-next-to-next-to-leading-order are available [5]. These corrections are of relative orders $\mathcal{O}(\alpha_s^n)$ with $n = 1, 2, 3$, respectively, in the strong-coupling constant α_s. The one-loop electroweak corrections, of relative order $\mathcal{O}(\alpha)$ in Sommerfeld's fine-structure constant α, were studied for the W boson in Ref. [6] and for the Z boson in Ref. [7]. At the mixed two-loop order $\mathcal{O}(\alpha\alpha_s)$, the corrections to the $q\bar{q}Z$ form factor were evaluated for light quarks $q \neq b, t$ in Ref. [8] using the techniques developed in Ref. [9], and the treatment of the nonfactorizable corrections in the resonance region was discussed in Ref. [10].

In order for the W and Z bosons to acquire finite transverse momenta (p_T), they must be produced in association with additional particles or hadron jets (j). The QCD corrections to the p_T distributions of W- and Z-boson inclusive hadroproduction were computed at NLO [11,12] and partly at NNLO [13]. The $\mathcal{O}(\alpha)$ corrections were investigated for the W boson in Refs. [14,15] and for the Z boson in Refs. [16,17]. Specifically, in Ref. [14], the electroweak $\mathcal{O}(\alpha)$ corrections to the $\mathcal{O}(\alpha\alpha_s)$ partonic subprocesses of W-boson production were calculated imposing a minimum-transverse-momentum cut on outgoing gluons to prevent soft-gluon singularities. However, this cut was not applied to outgoing quarks and antiquarks as well, which renders it impractical at the hadron level, where gluon and light-quark jets are hard to distinguish on an event-by-event basis. Such a cut is also problematic from the conceptual point of view because, as a matter of principle, a collinear gluon-photon system cannot be distinguished from a single gluon with the same momentum. In Ref. [15], the results of Ref. [14] were confirmed, but the soft-gluon singularities were properly eliminated by including also the $\mathcal{O}(\alpha_s)$ corrections to the $\mathcal{O}(\alpha^2)$ partonic subprocesses. Furthermore, the $\mathcal{O}(\alpha^3)$ contributions due to direct and resolved photoproduction by elastic and inelastic scattering off the incoming (anti)proton

were taken into account in Ref. [15].

In contrast to the charged-current case, the separation of the electroweak $\mathcal{O}(\alpha)$ corrections to the neutral-current Drell–Yan process into an electromagnetic and a weak part is meaningful with regard to infrared (IR) and ultraviolet (UV) finiteness and gauge independence. In Refs. [16,17], the purely weak $\mathcal{O}(\alpha)$ corrections to the $\mathcal{O}(\alpha\alpha_s)$ partonic subprocess $q\bar{q} \to Zg$ and its crossed versions were computed. They make up an important subset of the contributions of absolute order $\mathcal{O}(\alpha^2\alpha_s)$ to the inclusive hadroproduction of finite-p_T Z bosons. It is the purpose of this work to complete our knowledge of these contributions, which have several sources, and to check the results presented in Ref. [17]. To start with, we need to complement the purely weak $\mathcal{O}(\alpha)$ corrections to the $\mathcal{O}(\alpha\alpha_s)$ partonic subprocess $q\bar{q} \to Zg$ and its crossed versions by the QED ones, which have virtual and real parts. The $\mathcal{O}(\alpha^2\alpha_s)$ partonic subprocesses that we are then led to consider include $q\bar{q} \to Zg\gamma$. As in the charged-current case [15], we thus inevitably encounter a soft-gluon singularity. To cancel it, we need to also include the $\mathcal{O}(\alpha_s)$ QCD corrections to the $\mathcal{O}(\alpha^2)$ partonic subprocess $q\bar{q} \to Z\gamma$. Furthermore, $\mathcal{O}(\alpha^2\alpha_s)$ contributions may also arise from interferences of $\mathcal{O}(\alpha^{1/2}\alpha_s)$ and $\mathcal{O}(\alpha^{3/2})$ Feynman diagrams yielding a single Dirac spinor trace with nonvanishing color factor $\operatorname{tr} T^a T^a = N_c C_F$. This happens for the partonic subprocess $q\bar{q} \to Zq\bar{q}$ when a diagram involving a virtual gluon in the s (t) channel is connected with a diagram involving a photon or a Z boson in the t (s) channel, and for the subprocesses $qq \to Zqq$ and $\bar{q}\bar{q} \to Z\bar{q}\bar{q}$ when a gluon-exchange diagram and a photon/Z-boson-exchange diagram are connected with twisted quark lines. For completeness, we also recalculate the $\mathcal{O}(\alpha_s)$ QCD corrections to the inclusive hadroproduction of finite-p_T Z bosons [11,12] and thus recover the analytic results specified in Ref. [12] apart from a few misprints that we correct. Finally, we also study the leading-order (LO) photon-induced subprocesses, of order $\mathcal{O}(\alpha^2)$, which, after convolution with the photon PDFs of the (anti)proton, yield contributions of absolute order $\mathcal{O}(\alpha^3)$. As in Refs. [12,17], we list full analytic results in a compact form.

Our goal is to study the inclusive hadroproduction of single Z bosons with finite values of p_T. For the experimental analysis, this implies that all events with at least one identified Z boson are selected and sampled in bins of one or more kinematic variables exclusively pertaining to the Z boson, such as p_T and rapidity y. If there is more than one identified Z boson in such an event, then each of them generates one entry in the considered histogram. There is no need to identify particles of other species or jets that are produced in association with the Z bosons. If such additional experimental information is available, it is nevertheless ignored. Samples of events with at least one identified Z boson may, of course, also be analyzed more exclusively. For instance, one may study the production of a large-p_T Z boson in association with a jet or a prompt photon. The separation of $Z + j$ and $Z + \gamma$ events is efficiently achieved by means of the procedures elaborated in studies of the photon fragmentation function [18] and of photon isolation [19]. The contributions from $Z + X$ final states, in which the system X contains a heavy particle, e.g. a W, Z, or Higgs boson or a top quark, are greatly suppressed and not considered here.

The $\mathcal{O}(\alpha)$ corrections to $l^+\nu + j$, $l^+l^- + j$, and $\nu\bar{\nu} + j$ inclusive hadroproduction were

3

considered in Refs. [20,21,22], respectively. The theoretical study of such final states is closer to the experimental situation, as it does not rely on the identification of the W and Z bosons and the reconstruction of their four-momenta. The latter two procedures have been routinely applied in experimental data analyses ever since the discovery of the W and Z bosons at the SPS in 1983. They are, of course, subject to certain experimental errors, which are, however, quite small for the gold-plated $Z \to e^+e^-$ and $Z \to \mu^+\mu^-$ decay modes of relevance here. By the same token, the numerical results presented in Ref. [21] do not allow one to extract the p_T distribution of the Z boson and thus cannot be usefully compared with the results obtained in Refs. [16,17] and here. This would require kinematic cuts to reduce the contributions due to the nonresonant parts of the scattering amplitudes in Ref. [21] in analogy to the experimental acceptance cuts, e.g. the one confining the invariant mass M_{ll} of the l^+l^- pair to an appropriately narrow interval about M_Z. Apart from that, in Ref. [21], the cross sections were not presented as distributions in the transverse momentum of the l^+l^- pair, which could be identified with the kinematic variable p_T of the Z boson for the sake of a comparison with the results obtained in Refs. [16,17] and here. On the other hand, the M_{ll} distributions shown in Figs. 7 and 8 of Ref. [21] exhibit a rapid fall-off at the shoulders of the peak at $M_{ll} = M_Z$ indicating that the narrow-width approximation adopted in Refs. [16,17] and here is quite appropriate for the Tevatron and the LHC. The $\mathcal{O}(\alpha^2\alpha_s)$ interference contributions mentioned above were neglected in Refs. [21,22] appealing to the observation that similar contributions were found to be numerically small in Ref. [20]. Recently, $\mathcal{O}(\alpha)$ corrections were also calculated for the hadroproduction of the final states $l^+l^- + 2j$ [23] and $W^+ + nj$ with $n = 1, 2, 3$ [24].

This paper is organized as follows. In Sec. 2, we explain our analytic calculations. In Sec. 3, we present our numerical results. Our conclusions are contained in Sec. 4. Our analytic results are listed in Appendices A–C.

2 Analytic results

We consider the inclusive production of a Z boson in the collision of two hadrons h_1 and h_2,

$$h_1(P_1) + h_2(P_2) \to Z(q) + X, \tag{1}$$

where the four-momenta are indicated in parentheses and X collectively denotes the residual particles in the final state. We take the Z boson to be on mass shell, $q^2 = M_Z^2$, neglect the hadron masses, $P_1^2 = P_2^2 = 0$, and define the hadronic Mandelstam variables as

$$S = (P_1 + P_2)^2, \qquad T = (P_1 - q)^2, \qquad U = (P_2 - q)^2, \qquad Q^2 = q^2. \tag{2}$$

In the center-of-mass frame, we write $q^\mu = (q^0, \mathbf{q}_T, q^3)$, where $\mathbf{q}_T$ is the transverse momentum, and define $q_T = |\mathbf{q}_T|$ and the rapidity $y = (1/2)\ln[(q^0 + q^3)/(q^0 - q^3)]$. Using Eq. (2), we have

$$q_T^2 = \frac{TU - Q^2(S + T + U - Q^2)}{S}, \qquad y = \frac{1}{2}\ln\frac{U - Q^2}{T - Q^2}. \tag{3}$$

We work in the collinear parton model of QCD with $n_f = 5$ massless quark flavors. We write the partonic subprocesses that contribute to the hadronic reaction in Eq. (1) generically as

$$i(p_1) + j(p_2) \to Z(q) + X(p_X), \tag{4}$$

where $p_i = x_i P_i$ with $i = 1, 2$. The partonic Mandelstam variables are defined as

$$s = (p_1 + p_2)^2, \qquad t = (p_1 - q)^2, \qquad u = (p_2 - q)^2, \qquad Q^2 = q^2, \qquad s_2 = p_X^2, \tag{5}$$

and satisfy

$$s + t + u = Q^2 + s_2. \tag{6}$$

The hadronic and partonic Mandelstam variables are related as follows:

$$s = x_1 x_2 S, \qquad t = x_1(T - Q^2) + Q^2, \qquad u = x_2(U - Q^2) + Q^2,$$
$$s_2 = x_1 x_2 S + x_1(T - Q^2) + x_2(U - Q^2) + Q^2. \tag{7}$$

The differential cross section for reaction (1) may be evaluated according to

$$\frac{d\sigma}{dq_T^2 \, dy} = \sum_{ij} \int dx_1 \, dx_2 \, f_{i/h_1}(x_1, \mu_F^2) f_{j/h_2}(x_2, \mu_F^2) \frac{s \, d\sigma_{ij}}{dt \, du}(x_1 P_1, x_2 P_2, \mu_F^2), \tag{8}$$

where the sum runs over all the partons i and j; $f_{i/h}(x, \mu_F^2)$ is the PDF of parton i in hadron h; and μ_F is the factorization scale. The partonic cross sections $d\sigma_{ij}/(dt\,du)$ may be computed in perturbation theory as double series in α_s and α. Apart from the Feynman rules of QCD, we also need those for the couplings of a quark q to the photon γ and the Z boson. They are given by the vertices $ieQ_q\gamma_\mu$ and $ie\gamma_\mu(v_q - \gamma_5 a_q)$, respectively, where Q_q is the electric charge of q in units of the positron charge $e = \sqrt{4\pi\alpha}$,

$$v_q = \frac{I_3 - 2Q_q \sin^2\theta_w}{2\sin\theta_w \cos\theta_w}, \qquad a_q = \frac{I_3}{2\sin\theta_w \cos\theta_w} \tag{9}$$

are its vector and axial vector couplings to the Z boson, I_3 is its third component of weak isospin, and θ_w is the weak mixing angle.

In the remainder of this section, we list the relevant partonic subprocesses with the contributing Feynman diagrams and outline the computation and its organization. At LO, we consider the $2 \to 2$ subprocesses

$$q + \bar{q} \to Z + g, \tag{10}$$
$$q + \bar{q} \to Z + \gamma, \tag{11}$$
$$q + g \to Z + q, \tag{12}$$
$$q + \gamma \to Z + q, \tag{13}$$

where it is understood that q may also be an antiquark, in which case $\bar{q}$ is a quark. They are mediated by the Feynman diagrams depicted in Fig. 1. At LO, subprocesses (10) and (12) are of $\mathcal{O}(\alpha\alpha_s)$, and suprocesses (11) and (13) are of $\mathcal{O}(\alpha^2)$.
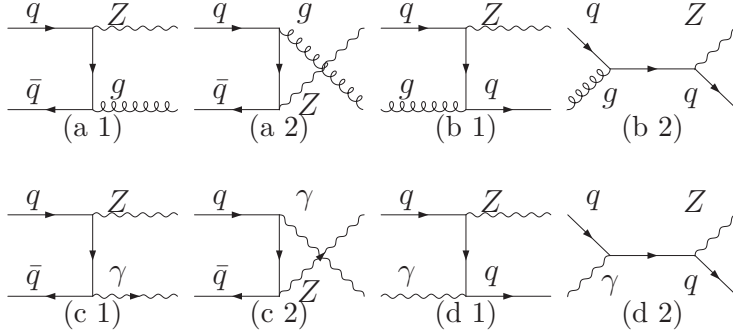
Figure 1: Tree-level diagrams contributing to the partonic subprocesses $q + \bar{q} \to Z + g$ and $q + g \to Z + q$ at $\mathcal{O}(\alpha\alpha_s)$ and to the partonic subprocesses $q + \bar{q} \to Z + \gamma$ and $q + \gamma \to Z + q$ at $\mathcal{O}(\alpha^2)$.

We include the $\mathcal{O}(\alpha_s)$ QCD corrections to subprocesses (10)–(12) and the $\mathcal{O}(\alpha)$ electroweak corrections to subprocesses (10) and (12), while we treat subprocess (13) only at LO because of the additional $\mathcal{O}(\alpha)$ suppression due to the photon emission by the incoming hadrons. The virtual QCD corrections to subprocesses (10) and (11) and the virtual QED corrections to subprocess (10) arise from the Feynman diagrams in Fig. 2. The virtual QCD and QED corrections to subprocess (12) are obtained by appropriately crossing external legs. The virtual weak corrections to subprocess (10) arise from the Feynman diagrams in Fig. 3, and those to subprocess (12) emerge by crossing.

The real QCD and QED corrections arise from the $2 \to 3$ subprocesses

$$q + \bar{q} \to Z + q + \bar{q}, \tag{14}$$
$$q + \bar{q} \to Z + q' + \bar{q}', \tag{15}$$
$$q + \bar{q} \to Z + g + g, \tag{16}$$
$$q + \bar{q} \to Z + g + \gamma, \tag{17}$$
$$q + q \to Z + q + q, \tag{18}$$
$$q + q' \to Z + q + q', \tag{19}$$
$$q + g \to Z + q + g, \tag{20}$$
$$q + g \to Z + q + \gamma, \tag{21}$$
$$g + g \to Z + q + \bar{q}, \tag{22}$$

where $q' \neq q$. Subprocesses (14) and (18) contribute both at $\mathcal{O}(\alpha\alpha_s^2)$ and $\mathcal{O}(\alpha^2\alpha_s)$, subprocesses (15), (16), (19), (20), and (22) contribute at $\mathcal{O}(\alpha\alpha_s^2)$, and subprocesses (17) and (21) contribute at $\mathcal{O}(\alpha^2\alpha_s)$. The tree-level diagrams contributing to subprocess (14) are shown in Fig. 4, those contributing to subprocesses (16) and (17) in Fig. 5, and those contributing to subprocesses (18) and (19) in Fig. 6.

As already mentioned in Sec. 1, the $\mathcal{O}(\alpha^2\alpha_s)$ contributions to subprocesses (14) and (18) are generated by interferences of $2 \to 3$ tree-level diagrams with a virtual gluon in one

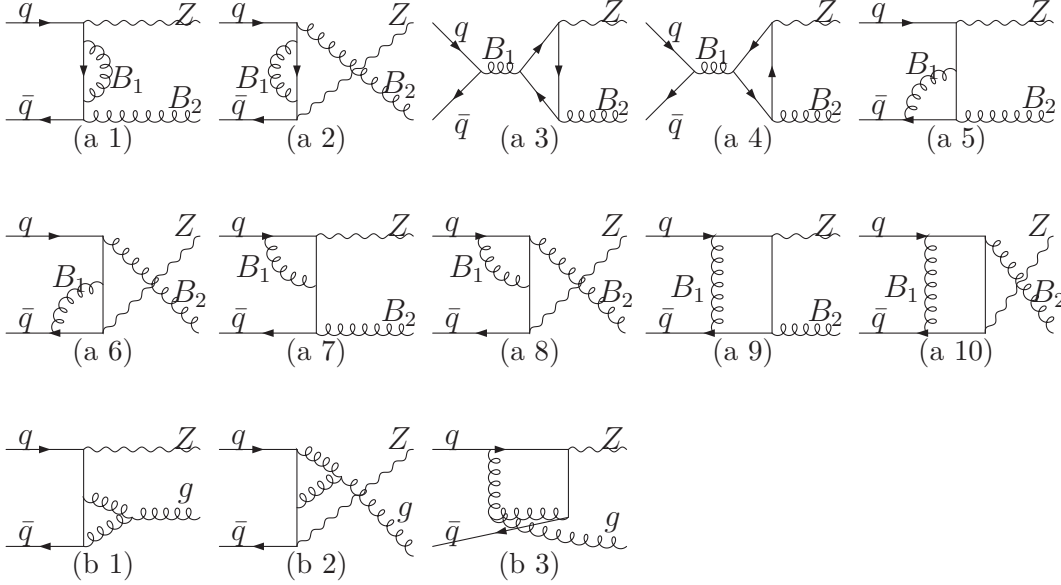Figure 2: QCD and QED one-loop diagrams contributing to the partonic subprocess $q+\bar{q} \to Z+g$ at $\mathcal{O}(\alpha\alpha_s^2)$ ($B_1 = B_2 = g$) and $\mathcal{O}(\alpha^2\alpha_s)$ (diagrams (a 1)–(a 10) with $B_1 = \gamma$ and $B_2 = g$) and to the partonic subprocess $q + \bar{q} \to Z + \gamma$ at $\mathcal{O}(\alpha^2\alpha_s)$ (diagrams (a 1)–(a 10) with $B_1 = g$ and $B_2 = \gamma$). The QCD and QED one-loop diagrams contributing to the partonic subprocess $q + g \to Z + q$ at $\mathcal{O}(\alpha\alpha_s^2)$ and $\mathcal{O}(\alpha^2\alpha_s)$ are obtained by appropriately crossing external legs.

factor and a virtual photon or Z boson in the other one in such a way that one closed quark line is formed yielding a nonvanishing color factor, $\operatorname{tr} T^a T^a = N_c C_F$, as indicated in Fig. 7. In the case of subprocess (14), this is achieved when the gluon is in the s channel and the photon or Z boson is in the t channel or vice versa. In the case of subprocess (18), this is achieved by twisting the quark lines in one of the interfering diagrams. These interference contributions exhaust the $\mathcal{O}(\alpha^2\alpha_s)$ corrections to subprocesses (14) and (18) and are thus finite and gauge-independent by themselves. On the other hand, interferences leading to two closed quark lines are nullified by $(\operatorname{tr} T^a)^2 = 0$. This explains, why subprocesses (15) and (19) do not receive $\mathcal{O}(\alpha^2\alpha_s)$ contributions. Obviously, these types of mixed QCD-QED corrections may not be obtained by merely manipulating coupling constants and color factors as is often the case for pure QED corrections.

We compute the full $\mathcal{O}(\alpha\alpha_s^2)$ and $\mathcal{O}(\alpha^2\alpha_s)$ corrections to the cross section of the hadronic process (1) according to Eq. (8) by including all the partonic subprocesses (10)–(22). We regularize both the UV and IR divergences using dimensional regularization in $D = 4 - 2\varepsilon$ space-time dimensions. The UV divergences arise from the $2 \to 2$ one-loop diagrams and are removed by renormalizing the coupling constants, masses, and wave functions in the respective $2 \to 2$ tree-level diagrams. We renormalize α_s and α

according to the modified minimal-subtraction ($\overline{\text{MS}}$) scheme and employ the electroweak on-shell renormalization scheme otherwise. In particular, we define θ_w in terms of the pole masses as $\cos\theta_w = M_W/M_Z$. The IR divergences, both of soft and collinear types, are generated by $2 \to 2$ one-loop and $2 \to 3$ tree-level diagrams. The soft and collinear divergences related to the final states are canceled by integrating over the kinematic degrees of freedom of the three-particle phase space that are related to the systems X and combining the outcome with the virtual corrections. Specifically, the three-particle kinematics turns into the two-particle one by taking the limit $s_2 \to 0$. This is implemented in dimensional regularization using the relationship

$$\frac{1}{s_2^{1+\varepsilon}} = \delta(s_2)\left(-\frac{1}{\varepsilon} + \ln s_2^{\text{max}} - \frac{\varepsilon}{2}\ln^2 s_2^{\text{max}} + \cdots\right) + \left(\frac{1}{s_2}\right)_+ + \left(\frac{\ln s_2}{s_2}\right)_+ + \cdots, \quad (23)$$

where s_2^{max} is the maximum value of s_2 allowed for given values of p_T and y and the plus distributions are defined for smooth test functions $f(s_2)$ as

$$\int_0^{s_2^{\text{max}}} ds_2 \left(\frac{1}{s_2}\right)_+ f(s_2) = \int_0^{s_2^{\text{max}}} ds_2 \frac{1}{s_2}[f(s_2) - f(0)],$$
$$\int_0^{s_2^{\text{max}}} ds_2 \left(\frac{\ln s_2}{s_2}\right)_+ f(s_2) = \int_0^{s_2^{\text{max}}} ds_2 \frac{\ln s_2}{s_2}[f(s_2) - f(0)]. \quad (24)$$

There remain collinear divergences related to the initial states, which are universal and are absorbed into the bare PDFs so to render them finite. In the $\overline{\text{MS}}$ factorization scheme, this PDF renormalization is implemented in the QCD sector as

$$f_{i/h}(x, \mu_F^2) = \sum_j \int_x^1 \frac{dy}{y} f_{j/h}^{\text{bare}}\left(\frac{x}{y}\right)\left[\delta_{ij}\delta(1-y) - \frac{\mu_F^{-2\varepsilon}}{\varepsilon}\frac{\alpha_s}{2\pi}\frac{\Gamma(1-\varepsilon)}{\Gamma(1-2\varepsilon)}P_{ij}(y) + \cdots\right], \quad (25)$$

where $P_{ij}(y)$ are the $j \to i$ splitting functions. In the one-loop approximation of QCD, the latter read [25]

$$P_{qq}(y) = C_F\left[\frac{3}{2}\delta(1-y) + 2\left(\frac{1}{1-y}\right)_+ - 1 - y\right],$$
$$P_{gq}(y) = C_F\frac{1 + (1-y)^2}{y},$$
$$P_{gg}(y) = \left(\frac{11}{6}C_A - \frac{2}{3}Tn_f\right)\delta(1-y) + 2C_A\left[\left(\frac{1}{1-y}\right)_+ + \frac{1}{y} - 2 + y(1-y)\right],$$
$$P_{qg}(y) = T[y^2 + (1-y)^2], \quad (26)$$

where $C_F = (N_c^2 - 1)/(2N_c) = 4/3$, $C_A = N_c = 3$, $T = 1/2$, and $n_f = 5$ is the number of active quark flavors. For simplicity, we adopt the $\overline{\text{MS}}$ factorization scheme also for the QED sector. The appropriate counterparts of Eqs. (25) and (26) are obtained by substituting $\alpha_s \to \alpha Q_q^2$, $C_F \to 1$, and $C_A \to 0$. Of course, the PDFs to be used in the

numerical analysis must then be implemented with the $\overline{\text{MS}}$ factorization scheme as well, both in their QCD and QED sectors. While the $\overline{\text{MS}}$ factorization scheme is now common standard for the QCD sector, alternative choices have been advocated for the QED sector, e.g. in connection with neutrino-nucleus deep-inelastic scattering (DIS), a DIS-like choice [26].

To exploit Eq. (23), it is useful to introduce s_2 as an integration variable in Eq. (8), in lieu of x_2, say. This leads to

$$\frac{d\sigma}{dq_T^2 \, dy} = \sum_{i,j} \int_{x_1^{\min}}^{1} dx_1 \int_{0}^{s_2^{\max}} \frac{ds_2}{x_1 S + U - Q^2} f_{i/h_1}(x_1, \mu_F^2) f_{j/h_2}(x_2, \mu_F^2) \frac{s \, d\sigma_{ij}}{dt \, du}(x_1 P_1, x_2 P_2, \mu_F^2),$$

(27)

where

$$x_1^{\min} = \frac{-U}{S + T - Q^2}, \qquad s_2^{\max} = U + x_1(S + T - Q^2), \qquad x_2 = \frac{s_2 - Q^2 - x_1(T - Q^2)}{x_1 S + U - Q^2},$$

$$T = Q^2 - e^{-y}\sqrt{S(Q^2 + q_T^2)}, \qquad U = Q^2 - e^{y}\sqrt{S(Q^2 + q_T^2)}.$$

(28)

At this point, we compare our analytic results with the literature [12,17]. The NLO QCD corrections, of relative order $\mathcal{O}(\alpha_s)$, due to the virtual contributions from subprocesses (10) and (12), and the real contributions from subprocesses (14)–(16), (18)–(20), and (22) are listed in Ref. [12]. Apart from some misprints,[1] we find agreement with Ref. [12]. The weak $\mathcal{O}(\alpha)$ corrections to subprocess (10) are listed in Ref. [17]. In Ref. [17], collinear divergences arising from box diagrams in intermediate steps of the calculation are regularized by introducing an infinitesimal quark mass λ, while we employ dimensional regularization. The λ-dependent one-loop scalar box integrals J_{12}, J_{13}, and J_{14} in Eq. (39) of Ref. [17] may be conveniently converted to dimensional regularization using the results of Ref. [27]. In Ref. [17], the renormalization is performed both in the $\overline{\text{MS}}$ scheme and in the on-shell scheme implemented with some running fine-structure constant as explained in Eqs. (49) and (50) of Ref. [17], which differs from the pure $\overline{\text{MS}}$ definition. Specifically, in the counterterm of the electromagnetic coupling constant, the photon self-energy, which appears there with argument $q^2 = 0$ in the pure on-shell scheme, is split into the fermionic and bosonic parts, and the argument of the former is shifted to $q^2 = M_Z^2$. While the latter construction is well defined at one loop, it becomes ambiguous at higher orders because of the required separation of fermionic and bosonic contributions, and it is bound to render the running fine-structure constant thus defined gauge dependent. By contrast, we work in a hybrid renormalization scheme, which uses the pure $\overline{\text{MS}}$ definition of α, but the electroweak on-shell scheme otherwise. Taking these conceptual differences into account, we fully agree with Ref. [17].

---

[1]In Eq. (2.12) of Ref. [12], $B_2^{qG}(s, t, u, Q^2)$ should be replaced with $\left[B_2^{qG}(s, t, u, Q^2) + C_2^{qG}(s, t, u, Q^2) \right]$ and $C_2^{qG}(s, t, u, Q^2)$ with $C_3^{qG}(s, t, u, Q^2)$.

In this paper, we only list those analytic results that may not be found in the previous literature. Specifically, we consider $\mathcal{O}(\alpha^2\alpha_s)$ contributions to $q+\bar{q} \to Z+X$, $q+g \to Z+X$, and $q+q \to Z+X$ in Appendices A, B, and C, respectively. In the case of $q+\bar{q} \to Z+X$, this includes the virtual QED corrections to subprocess (10), the virtual QCD corrections to subprocess (11), the real corrections from subprocess (17), and the above-mentioned interference contributions from subprocess (14). In the case of $q+g \to Z+X$, this includes the virtual QED corrections to subprocess (12) and the real corrections from subprocess (21). In the case of $q + q \to Z + X$, this includes the above-mentioned interference contributions from subprocess (18).

As already mentioned in Sec. 1, we also include the LO contributions from photoproduction. Incoming photons can participate in the hard scattering either directly or indirectly, i.e. through their quark and gluon content. The contributions from direct and resolved photoproduction are formally of the same order in the perturbative expansion. This may be understood by observing that the PDFs of the photon have a leading behavior proportional to $\alpha \ln(\mu_F^2/\Lambda_{\mathrm{QCD}}^2) \propto \alpha/\alpha_s(\mu_F^2)$, where Λ_{QCD} is the asymptotic scale parameter of QCD. At LO, direct photoproduction proceeds via subprocess (13) and resolved photoproduction via subprocesses (10) and (12). The cross section of subprocess (13) reads [28]

$$\frac{d\sigma_{q\gamma}}{dt} = -\frac{2\pi\alpha^2 Q_q^2(v_q^2 + a_q^2)}{N_c s^2}\left(\frac{t}{s} + \frac{s}{t} + \frac{2uQ^2}{st}\right), \tag{29}$$

where the Mandelstam variables and gauge coupling constants are defined in Eqs. (5) and (9), respectively. The ones of subprocesses (10) and (12) may be read off from Eqs. (30) and (39), respectively. The emission of photons off the (anti)proton can happen either elastically or inelastically, i.e. the (anti)proton stays intact or is destroyed, respectively. In both cases, an appropriate PDF can be evaluated in the Weizsäcker-Williams approximation [29,30,31,32]. Since these PDFs are of $\mathcal{O}(\alpha)$, the LO photoproduction contributions are of $\mathcal{O}(\alpha^3)$. Although photoproduction contributions are parametrically suppressed by a factor of α/α_s relative to the $\mathcal{O}(\alpha^2\alpha_s)$ corrections discussed above, we include them in our analysis because they may turn out to be sizable in certain regions of phase space.

We generated the Feynman diagrams using the program package DIANA [33] and checked the output using the program package FeynArts 3 [34]. We reduced the one-loop tensor integrals to scalar ones using custom-made routines written with the symbolic manipulation program FORM version 4.0 [35]. We evaluated the scalar one-loop integrals using the analytic results listed in Ref. [27].

3   Numerical analysis

We are now in a position to present our numerical analysis. As input we use the pole masses $M_W = 80.385$ GeV, $M_Z = 91.1876$ GeV, $M_H = 125$ GeV, $m_b = 4.89$ GeV, and $m_t = 173.07$ GeV, and the $\overline{\mathrm{MS}}$ coupling constants $\bar{\alpha}(M_Z^2) = 1/127.944$ [36] and $\alpha_s^{(5)}(M_Z^2) = 0.1180$ [32] to gauge $\bar{\alpha}(\mu_R^2)$ and $\alpha_s^{(5)}(\mu_R^2)$. We employ the NNPDF2.3QED NLO set of proton PDFs [32], which also include QED evolution and provide a photon

distribution function. This allows us to consistently treat direct and resolved photoproduction via inelastic scattering off the (anti)proton along with ordinary hadroproduction. In Ref. [32], the QED sector is treated at LO, or, more accurately, at the leading logarithmic level, where factorization is still trivial and does not yet require the specification of a scheme. In this sense, the NNPDF2.3QED NLO PDFs are compatible with our convention of employing the $\overline{\text{MS}}$ factorization scheme in the QED sector [37]. By the same token, the dependence on the QED factorization scheme contributes to the theoretical uncertainty, which we refrain from assessing here. As for photoproduction via elastic scattering off the (anti)proton, we adopt the photon flux function from Ref. [29] and the resolved-photon PDFs from Ref. [38]. For definiteness, we identify the renormalization and factorization scales with the Z-boson transverse mass, $\mu_R = \mu_F = \sqrt{p_T^2 + M_Z^2}$.

In Fig. 8, we study the cross section of $p\bar{p} \to Z + X$ at center-of-mass energy $\sqrt{S} = 1.96$ TeV appropriate for Tevatron run II (a) differential in p_T integrated over y and (b) differential in y imposing the acceptance cut $p_T > 10$ GeV. Specifically, we show (i) the NLO QCD result considered in Ref. [12], i.e. the sum of the $\mathcal{O}(\alpha\alpha_s)$ and $\mathcal{O}(\alpha\alpha_s^2)$ results (thin solid lines); (ii) the $\mathcal{O}(\alpha^2)$ Born result (thin dot-dashed lines); (iii) the purely weak $\mathcal{O}(\alpha^2\alpha_s)$ corrections to subprocesses (10) and (12) considered in Ref. [17] (thick dashed green lines); (iv) the residual electroweak $\mathcal{O}(\alpha^2\alpha_s)$ corrections (thin dashed blue lines); (v) the $\mathcal{O}(\alpha^3)$ photoproduction contributions (thin dotted blue lines); and (vi) the total sum (thick solid red lines). The p_T distributions in Fig. 8(a) are plotted on a logarithmic scale. Since the one of contribution (iii) is negative in the considered p_T range, its modulus is shown. The y distributions in Fig. 8(b) are plotted on a linear scale. For better visibility, contributions (ii), (iv), and (v) are amplified by a factor of 100. In Fig. 8(b), we do not consider negative y values because the y distributions are symmetric by charge conjugation invariance. In Fig. 9, we decompose contribution (iv) (thick solid red lines) into the combination of the $\mathcal{O}(\alpha)$ QED corrections to subprocesses (10) and (12) and the $\mathcal{O}(\alpha_s)$ QCD corrections to subprocess (11) (thin solid lines), which cannot be usefully separated, and the QCD-electroweak interference contributions from subprocesses (14) (thin dot-dashed lines) and (18) (thin dashed green lines). In Figs. 10 and 11, we repeat the analyses of Figs. 8 and 9, respectively, for $pp \to Z + X$ at $\sqrt{S} = 14$ TeV appropriate for the LHC.

From Figs. 8 and 10, we observe that the combined effect of the electroweak contributions (ii)–(v) is to reduce the NLO QCD predictions (i). The reduction ranges from a few percent at low p_T values to a few tens of percent in the large-p_T domain, where large Sudakov logarithms dominate. The bulk of the electroweak contributions (ii)–(v) is made up by the purely weak $\mathcal{O}(\alpha^2\alpha_s)$ corrections to subprocesses (10) and (12) [contribution (iii)], which are negative throughout the kinematic ranges considered here. The residual types of electroweak effects taken into accout here, namely the $\mathcal{O}(\alpha^2)$ Born result (ii), the residual electroweak $\mathcal{O}(\alpha^2\alpha_s)$ corrections (iv), and the $\mathcal{O}(\alpha^3)$ photoproduction contributions (v), are all positive, but numerically suppressed by typically one order of magnitude or more relative to contribution (iii), except for contribution (ii) in the small-p_T range.

In Fig. 9(a), the QED-type correction is throughout positive, the $q\bar{q}$ interference contribution is throughout negative, and the qq interference contribution is negative for

$p_T \gtrsim 165$ GeV. On the other hand, in Fig. 11(a), the QED-type correction is negative for $p_T \gtrsim 480$ GeV, the $q\bar{q}$ interference contribution is again throughout negative, and the qq interference contribution is throughout positive. From Figs. 9(a) and 11(a), we observe that those two interference contributions are suppressed relative to the QED-type correction in the small-p_T range. This is also reflected in the y distributions of Figs. 9(b) and 11(b), which receive dominant contributions from the small-p_T ranges. Such a suppression is expected from the comparison of color factors [21,22]. However, the situation is quite different at large p_T values. In fact, in Fig. 9(a), the $q\bar{q}$ interference contribution steadily approaches the QED-type contribution for increasing value of p_T, and, in Fig. 11(a), the qq interference contribution exceeds the QED-type contribution for $p_T \gtrsim 300$ GeV. Comparing Figs. 9 and 11 with Figs. 8 and 10, we observe that the three $\mathcal{O}(\alpha^2 \alpha_s)$ contributions of class (iv) range at the permille level with respect to the well-known NLO QCD result [12]. Specifically, in the case of σ/dy at $y = 0$, the QED-type, qq interference, and $q\bar{q}$ interference contributions normalized to the NLO QCD result approximately amount to 3×10^{-3}, 2×10^{-4}, and -1×10^{-4} at the Tevatron and to 1×10^{-3}, 8×10^{-5}, and -2×10^{-4} at the LHC, respectively.

4   Conclusions

We studied the inclusive hadroproduction of large-p_T single Z bosons including both the QCD and electroweak NLO corrections and presented p_T and y distributions under Tevatron and LHC kinematic conditions. Our analytic results agree with the literature as far as the latter goes. Specifically, we recovered the well-known NLO QCD corrections [12], of absolute order $\mathcal{O}(\alpha \alpha_s^2)$, and the purely weak one-loop corrections, of absolute order $\mathcal{O}(\alpha^2 \alpha_s)$, to the partonic subprocess $q\bar{q} \to Zg$ and its crossed versions [17]. We completed our knowledge of the $\mathcal{O}(\alpha^2 \alpha_s)$ corrections by providing also the QED corrections and some missing weak contributions due to interferences of tree-level $2 \to 3$ scattering amplitudes in compact analytic form ready to be used by the interested reader. While the new $\mathcal{O}(\alpha^2 \alpha_s)$ contributions turned out to be numerically small, their knowledge should help us to reduce the theoretical uncertainty on this important benchmark cross section. We also considered, for the first time, direct and resolved photoproduction in elastic and inelastic scattering.

In the experimental analyses to be compared with our theoretical predictions, Z bosons must be identified, preferrably via their decays to $e^+ e^-$ or $\mu^+ \mu^-$ pairs, and their four-momenta must be reconstructed and sampled in bins of p_T or y, ignoring any other available information about the selected events. If there are more than one identified and reconstructed Z boson in an event, then each of them is taken to generate one entry in the considered histogram. Theoretical predictions for the hadroproduction of more exclusive final states, such as $l^+ l^- + j$ [21] or $\nu\bar{\nu} + j$ [22], require a different mode of experimental data analysis. In this sense, the results presented here are not already included in Refs. [21,22], the more so as QCD-electroweak interference contributions of the type mentioned above were neglected there. Our detailed study confirmed the expectation [21,22] based on

the analysis of $l^+\nu + j$ hadroproduction [20] that those interference contributions are numerically small, for the small-p_T regime.

Acknowledgments

A Cross section of $\bar{q} + q \to Z + X$ through $\mathcal{O}(\alpha^2 \alpha_s)$

In this appendix, we consider $\mathcal{O}(\alpha^2 \alpha_s)$ contributions to $\bar{q} + q \to Z + X$. This includes the virtual QED corrections to subprocess (10), the virtual QCD corrections to subprocess (11), the real corrections from subprocess (17), and the interference contributions from subprocess (14) involving a virtual photon or Z boson. We have

$$
\frac{s \, d\sigma^{\bar{q}q}}{dt \, du} = \frac{2\pi\alpha^2 Q_q^2 (v_q^2 + a_q^2)}{N_c s} \left[\delta(s_2) A_0 \right.
$$
$$
\left. + C_F \frac{\alpha_s}{\pi} \left(\delta(s_2) A_1 + A_2 + A_3 + \frac{v_q^4 + 6 v_q^2 a_q^2 + a_q^4}{v_q^2 + a_q^2} A_4 \right) \right], \tag{30}
$$

where

$$
A_0 = \frac{t}{u} + \frac{u}{t} + 2 \left(\frac{s}{t} + \frac{s}{u} + \frac{s^2}{tu} \right), \tag{31}
$$

$$
A_1 = A_0 \left[L_{\mu_F} (2L_t + 2L_u - 4L_A - 3) + 4L_A(L_A + L_s - L_t - L_u - 1) + (L_t + L_u)^2 \right]
$$
$$
+ L_s^2 \left(-\frac{2s^2}{tu} - A_0 \right) + L_s \left(\frac{8s}{t+u} + \frac{4s^2}{(t+u)^2} \right)
$$
$$
+ \left(2A_0 + \frac{4s^2}{tu} \right) \left(L_s \ln \frac{s - Q^2}{Q^2} - \mathrm{Li}_2 \left(\frac{Q^2}{s} \right) \right) + \zeta(2) \left(\frac{4s^2}{tu} + 8A_0 \right)
$$
$$
+ \left\{ L_t \left(\frac{t + 4s}{s+u} + \frac{st}{(s+u)^2} \right) + L_s L_t \left(\frac{2(2s+t)}{u} - 4A_0 \right) \right.
$$
$$
+ \frac{2(2s^2 + 2su + u^2)}{tu} \left(L_t \ln \frac{s+u}{Q^2} + \mathrm{Li}_2 \left(\frac{t}{Q^2} \right) \right)
$$
$$
\left. - \frac{9t + 17s}{u} - \frac{8s^2}{tu} + \frac{2s}{t+u} + \frac{s}{s+t} \right\} + \left\{ u \leftrightarrow t \right\}, \tag{32}
$$

$$A_2 = \left[4A_0\left(-\ln\frac{(s_2-t)(s_2-u)}{s^2} - L_{\mu_F} + 2\ln\frac{s_2}{Q^2} - L_s\right)\frac{1}{s_2}\right]_{A+}$$

$$+ \ln\frac{tu-Q^2 s_2}{(s_2-t)(s_2-u)}\left(\frac{4s^2(s-Q^2)}{tu(s_2-t)(s_2-u)} + \frac{2(2s+u-t)}{t(s_2-t)} + \frac{2(2s+t-u)}{u(s_2-u)}\right.$$

$$\left. + \frac{4Q^2 A_0 - 2u - 2t - 2Q^2 - 6s}{tu-Q^2 s_2} + \frac{2(t+u+s+Q^2)}{tu}\right)$$

$$+ \ln\frac{(s_2-t)(s_2-u)}{ss_2}\left(\frac{4s^2(s-Q^2)}{tu(s_2-t)(s_2-u)} + \frac{2(2s+u-t)}{t(s_2-t)} + \frac{2(2s+t-u)}{u(s_2-u)}\right)$$

$$+ \ln\frac{\mu_F^2}{s_2}\left(\frac{s}{(s_2-t)^2} + \frac{s}{(s_2-u)^2} - \frac{2s+u+t}{t(s_2-t)} - \frac{2s+t+u}{u(s_2-u)} + \frac{Q^2}{t^2} + \frac{Q^2}{u^2}\right.$$

$$\left. - \frac{4Q^2 A_0 - 2u - 2t - 2Q^2 - 6s}{tu-Q^2 s_2}\right)$$

$$+ \frac{s}{(s_2-t)^2} + \frac{s}{(s_2-u)^2} + \frac{2(u/t+s/t-s/u)}{s_2-t} + \frac{2(t/u+s/u-s/t)}{s_2-u}$$

$$+ \frac{2(s-Q^2+Q^2 u/t+Q^2 t/u)}{tu-Q^2 s_2} + \frac{2(t+u-s)}{tu} , \tag{33}$$

$$A_3 = \frac{1}{\lambda}L_\lambda\left(\frac{3s(t-u)^2(t+u)(4Q^2 s+(t+u)^2)}{2tu\lambda^4}\right.$$

$$- \frac{2s(t^3+u^3) + Q^2(-4s(t-u)^2 + 2s^2(t+u) - (t-u)^2(t+u))}{tu\lambda^2}$$

$$+ \frac{(t+u)(4s^2+t^2+u^2+2s(t+u))}{s_2 tu} + \frac{6(s-Q^2)(t^2+u^2)}{stu} + \frac{2(6s+t+u)}{s+Q^2-s2}$$

$$\left. + \frac{(9s-18Q^2+8Q^4/s)(t+u)}{2tu} + \frac{3(t^3+t^2 u+tu^2+u^3)}{stu} - \frac{4Q^2}{s} + 2\right)$$

$$+ \frac{1}{2st}L_{\lambda t}\left(\frac{4s^2+t^2+4su+u^2}{s+Q^2-s_2} + 2Q^2 - 4s - t - 3u\right)$$

$$+ \frac{1}{2su}L_{\lambda u}\left(\frac{4s^2+u^2+4st+t^2}{s+Q^2-s_2} + 2Q^2 - 4s - u - 3t\right)$$

$$+ \frac{1}{2t}L_{st}\left(\frac{-2s_2+3t+u}{s} + \frac{2(2s^2+2su+u^2)}{s_2 u}\right.$$

$$\left. - \frac{2(2s-2s_2+t+2u)}{t} + \frac{4s^2+t^2+4su+u^2}{s(s+Q^2-s_2)}\right)$$

$$+ \frac{1}{2u} L_{su} \left(\frac{-2s_2 + 3u + t}{s} + \frac{2(2s^2 + 2st + t^2)}{s_2 t} \right.$$

$$\left. - \frac{2(2s - 2s_2 + u + 2t)}{u} + \frac{4s^2 + u^2 + 4st + t^2}{s(s + Q^2 - s_2)} \right)$$

$$+ \frac{3(t - u)^2(t + u)(-2Q^2(2s + t + u) + (t + u)(4s + t + u))}{2tu\lambda^4}$$

$$- \frac{t^3 + t^2 u + tu^2 + u^3 - Q^2(t + u)(2s + t + u) + s(6t^2 - 4tu + 6u^2)}{tu\lambda^2}$$

$$+ \frac{s^2}{u(s_2 - t)^2} + \frac{s^2}{t(s_2 - u)^2} + \left(2 + \frac{3s^2}{tu} \right) \left(\frac{1}{s_2 - t} + \frac{1}{s_2 - u} \right)$$

$$+ \frac{1}{s} \left(\frac{1}{t^2} + \frac{1}{u^2} \right) \left(4Q^4 + 2tu - Q^2(7s + 4(t + u)) \right) + \frac{3s(t + u) - 4tu}{2stu} , \qquad (34)$$

$$A_4 = \frac{L_\lambda}{\lambda^5} \frac{3s(t - u)^2(t + u)}{4tu} \left(\frac{s(t + u)^2(s + s_2 - Q^2)}{(s - Q^2)(s_2 - Q^2)} + 4sQ^2 + (t + u)^2 \right)$$

$$+ \frac{L_\lambda}{\lambda^3} \left(\frac{s(-3t^3 + t^2 u + tu^2 - 3u^3) + Q^2(4s(t - u)^2 - 2s^2(t + u) + (t - u)^2(t + u))}{2tu} \right.$$

$$\left. - \frac{s^2(t^3 + t^2 u + tu^2 + u^3)}{2(s - Q^2)tu} + \frac{s((t^2 - u^2)^2 - 2s(t^3 + u^3))}{2tu(s_2 - Q^2)} \right)$$

$$+ \frac{L_\lambda}{\lambda} \left(-2 + 2\frac{s_2^2}{u(s - Q^2)} + \frac{s_2^2}{u(s_2 - Q^2)} + 2\frac{s_2^2}{t(s - Q^2)} + \frac{s_2^2}{t(s_2 - Q^2)} \right.$$

$$+ 2\frac{s_2^2}{su} + 2\frac{s_2^2}{st} - \frac{us_2}{t(s - Q^2)} - \frac{us_2}{t(s_2 - Q^2)} - 4\frac{us_2}{st} + \frac{1}{2}\frac{u^2}{t(s - Q^2)} + \frac{1}{2}\frac{u^2}{t(s_2 - Q^2)}$$

$$+ \frac{7}{2}\frac{u^2}{ts_2} - \frac{u^2}{s(s + Q^2 - s_2)} + \frac{7}{2}\frac{u^2}{st} - \frac{ts_2}{u(s - Q^2)} - \frac{ts_2}{u(s_2 - Q^2)} - 4\frac{ts_2}{su}$$

$$- 2\frac{tu}{s(s + Q^2 - s_2)} + \frac{1}{2}\frac{t^2}{u(s - Q^2)} + \frac{1}{2}\frac{t^2}{u(s_2 - Q^2)} + \frac{7}{2}\frac{t^2}{us_2} - \frac{t^2}{s(s + Q^2 - s_2)} + \frac{7}{2}\frac{t^2}{su}$$

$$- \frac{1}{2}\frac{ss_2}{u(s - Q^2)} - \frac{ss_2}{u(s_2 - Q^2)} - \frac{1}{2}\frac{ss_2}{t(s - Q^2)} - \frac{ss_2}{t(s_2 - Q^2)} + \frac{su}{(s + Q^2 - s_2)(s - Q^2)}$$

$$+ \frac{1}{2}\frac{su}{t(s - Q^2)} + \frac{1}{2}\frac{su}{t(s_2 - Q^2)} + 10\frac{su}{ts_2} + \frac{st}{(s + Q^2 - s_2)(s - Q^2)} + \frac{1}{2}\frac{st}{u(s - Q^2)}$$

$$+ \frac{1}{2}\frac{st}{u(s_2 - Q^2)} + 10\frac{st}{us_2} + 6\frac{s^2}{(s + Q^2 - s_2)(s - Q^2)} + \frac{3}{4}\frac{s^2}{u(s - Q^2)} + \frac{9}{4}\frac{s^2}{u(s_2 - Q^2)}$$

$$+ 8\frac{s^2}{us_2} + \frac{3}{4}\frac{s^2}{t(s - Q^2)} + \frac{9}{4}\frac{s^2}{t(s_2 - Q^2)} + 8\frac{s^2}{ts_2} - \frac{17}{4}\frac{s}{t} - \frac{17}{4}\frac{s}{u} + 20\frac{s}{s_2}$$

$$+6\frac{s}{(s+Q^2-s_2)}+3\frac{s}{(s_2-Q^2)}+\frac{9}{2}\frac{t}{s}+\frac{3}{2}\frac{t}{u}+\frac{19}{2}\frac{t}{s_2}+3\frac{t}{(s+Q^2-s_2)}+\frac{1}{2}\frac{t}{(s_2-Q^2)}$$

$$+\frac{5}{2}\frac{t}{(s-Q^2)}+\frac{9}{2}\frac{u}{s}+\frac{3}{2}\frac{u}{t}+\frac{19}{2}\frac{u}{s_2}+3\frac{u}{(s+Q^2-s_2)}+\frac{1}{2}\frac{u}{(s_2-Q^2)}+\frac{5}{2}\frac{u}{(s-Q^2)}$$

$$-6\frac{s_2}{s}-\frac{3}{2}\frac{s_2}{t}-\frac{3}{2}\frac{s_2}{u}-2\frac{s_2}{(s_2-Q^2)}-6\frac{s_2}{(s-Q^2)}\Bigg)$$

$$+\frac{1}{\lambda^4}\frac{3(t-u)^2(t+u)}{4tu(Q^2-s)(s_2-Q^2)}\Bigg(4Q^6(2s+t+u)-4Q^4\Big(3s^2+6s(t+u)+(t+u)^2\Big)$$

$$+Q^2\Big(4s^3+28s^2(t+u)+14s(t+u)^2+(t+u)^3\Big)-s(t+u)\Big(8s^2+9s(t+u)$$

$$+2(t+u)^2\Big)\Bigg)+\frac{1}{\lambda^2}\frac{1}{4tu(s-Q^2)(s_2-Q^2)}\Bigg(4Q^6(t+u)(2s+t+u)$$

$$-4Q^4\Big(3s^2(t+u)+(t+u)^3+s(13t^2-2tu+13u^2)\Big)+Q^2\Big(4s^3(t+u)$$

$$+(t+u)^4+8s^2(9t^2-4tu+9u^2)+8s(4t^3+3t^2u+3tu^2+4u^3)\Big)$$

$$-s\Big(8s^2(3t^2-2tu+3u^2)+(t+u)^2(5t^2-2tu+5u^2)$$

$$+12s(2t^3+t^2u+tu^2+2u^3)\Big)\Bigg)\Bigg)$$

$$+2\frac{s_2^2}{u^2(s-Q^2)}+\frac{3}{2}\frac{s_2^2}{u^2(s_2-Q^2)}+2\frac{s_2^2}{t^2(s-Q^2)}$$

$$+\frac{3}{2}\frac{s_2^2}{t^2(s_2-Q^2)}-2\frac{us_2}{t^2(s-Q^2)}-\frac{3}{2}\frac{us_2}{t^2(s_2-Q^2)}-\frac{u^2}{t^2(s_2-t)}-2\frac{ts_2}{u^2(s-Q^2)}$$

$$-\frac{3}{2}\frac{ts_2}{u^2(s_2-Q^2)}-\frac{t^2}{u^2(s_2-u)}-2\frac{ss_2}{u^2(s-Q^2)}-\frac{3}{2}\frac{ss_2}{u^2(s_2-Q^2)}-2\frac{ss_2}{t^2(s-Q^2)}$$

$$-\frac{3}{2}\frac{ss_2}{t^2(s_2-Q^2)}-2\frac{su}{t^2(s_2-t)}-2\frac{st}{u^2(s_2-u)}+3\frac{s^2}{(s_2-u)^3}+3\frac{s^2}{(s_2-t)^3}$$

$$+\frac{s^2}{u(s_2-u)^2}+\frac{3}{2}\frac{s^2}{u(s_2-t)(s_2-Q^2)}-\frac{13}{2}\frac{s^2}{u(s_2-t)^2}-\frac{s^2}{u^2(s_2-u)}$$

$$+\frac{3}{2}\frac{s^2}{t(s_2-u)(s_2-Q^2)}-\frac{13}{2}\frac{s^2}{t(s_2-u)^2}+\frac{s^2}{t(s_2-t)^2}+3\frac{s^2}{tu(s_2-Q^2)}$$

$$+\frac{1}{2}\frac{s^2}{tu(s_2-u)}+\frac{1}{2}\frac{s^2}{tu(s_2-t)}-\frac{s^2}{t^2(s_2-t)}+\frac{1}{2}\frac{s^2s_2}{u(s_2-t)^2(s_2-Q^2)}$$

$$+\frac{1}{2}\frac{s^2s_2}{t(s_2-u)^2(s_2-Q^2)}+3\frac{s^3}{u(s_2-t)^3}+3\frac{s^3}{t(s_2-u)^3}+\frac{s^3}{tu(s_2-u)^2}$$

$$+\frac{s^3}{tu(s_2-t)^2}+\frac{s}{(s_2-u)(s-Q^2)}-4\frac{s}{(s_2-u)^2}+\frac{s}{(s_2-t)(s-Q^2)}$$

$$- 4\frac{s}{(s_2 - t)^2} + \frac{1}{4}\frac{s}{u(s - Q^2)} - \frac{1}{4}\frac{s}{u(s_2 - Q^2)} + 5\frac{s}{u(s_2 - t)} + \frac{1}{2}\frac{s}{u^2}$$

$$+ \frac{1}{4}\frac{s}{t(s - Q^2)} - \frac{1}{4}\frac{s}{t(s_2 - Q^2)} + 5\frac{s}{t(s_2 - u)} + \frac{1}{2}\frac{s}{t^2} + \frac{t}{u(s - Q^2)} + \frac{1}{4}\frac{t}{u(s_2 - Q^2)}$$

$$+ \frac{1}{2}\frac{t}{u^2} - 2\frac{t}{s^2} + \frac{u}{t(s - Q^2)} + \frac{1}{4}\frac{u}{t(s_2 - Q^2)} + \frac{1}{2}\frac{u}{t^2} - 2\frac{u}{s^2} - 2\frac{s_2}{u(s - Q^2)}$$

$$- \frac{s_2}{u(s_2 - Q^2)} + \frac{1}{2}\frac{s_2}{u^2} - 2\frac{s_2}{t(s - Q^2)} - \frac{s_2}{t(s_2 - Q^2)} + \frac{1}{2}\frac{s_2}{t^2} + 2\frac{s_2}{s^2} - 5\frac{1}{s} - \frac{3}{4}\frac{1}{t}$$

$$- \frac{3}{4}\frac{1}{u} + 2\frac{1}{(s_2 - t)} + 2\frac{1}{(s_2 - u)} - \frac{1}{2}\frac{1}{(s_2 - Q^2)} - \frac{1}{(s - Q^2)}$$

$$+ \left\{ L_t \left(\frac{t^2}{u^2(s_2 - u)} - \frac{t^3}{u^2(s_2 - u)^2} - 4\frac{st}{(s_2 - u)^3} + 2\frac{st}{u^2(s_2 - u)} - 3\frac{st^2}{u^2(s_2 - u)^2} \right.\right.$$

$$- 12\frac{s^2}{(s_2 - u)^3} + \frac{s^2}{u^2(s_2 - u)} + 8\frac{s^2}{t(s_2 - u)^2} - 4\frac{s^2}{tu(s_2 - u)} + 4\frac{s^2}{tus_2} + 3\frac{s^2t}{(s_2 - u)^4}$$

$$+ \frac{s^2t}{u(s_2 - u)^3} - 3\frac{s^2t}{u^2(s_2 - u)^2} + 6\frac{s^3}{(s_2 - u)^4} + 2\frac{s^3}{u(s_2 - u)^3} - \frac{s^3}{u^2(s_2 - u)^2}$$

$$- 8\frac{s^3}{t(s_2 - u)^3} + 3\frac{s^4}{t(s_2 - u)^4} + \frac{s^4}{tu(s_2 - u)^3} + 9\frac{s}{(s_2 - u)^2} - 4\frac{s}{u(s_2 - u)} + 6\frac{s}{us_2}$$

$$- 4\frac{s}{t(s_2 - u)} + 4\frac{s}{ts_2} + 2\frac{t}{(s_2 - u)^2} - \frac{t}{u(s_2 - u)} + \frac{5}{2}\frac{t}{us_2} + \frac{3}{2}\frac{t}{su} + \frac{u}{ts_2} - \frac{s_2}{su}$$

$$\left. + \frac{3}{2}\frac{1}{s} + \frac{1}{u} + 3\frac{1}{s_2} - 3\frac{1}{(s_2 - u)} \right) + L_{st} \left(\frac{2Q^2 + t - u}{4t(s - Q^2)} + \frac{4s^2 + t^2 + 4su + u^2}{4t(s - Q^2)(Q^2 + s - s_2)} \right.$$

$$\left. + \frac{2st(s + u) - 2s_2uQ^2 + tu^2}{2t^2u(s_2 - Q^2)} \right) + \frac{2s_2^2 - 2s_2t + t^2}{2t(s - Q^2)(Q^2 + s - s_2)} L_{\lambda t}$$

$$+ I_4(1, 1, t, -1) \left(\frac{4s^3 - u(t + u)^2 + 4s^2(t + 2u) + s(t^2 + 2tu + 3u^2)}{4s(Q^2 + s - s_2)} \right.$$

$$+ \frac{15}{2}s_2 - \frac{3}{4}u + \frac{13}{4}t + \frac{35}{2}s - 6\frac{s_2^2}{s} - 6\frac{s_2^2}{t} + \frac{s_2^2}{u} + 2\frac{s_2^3}{st} + \frac{23}{2}\frac{us_2}{s} + 10\frac{us_2}{t}$$

$$- 6\frac{us_2^2}{st} - \frac{23}{4}\frac{u^2}{s} - 2\frac{u^2}{t} - 8\frac{u^2}{s_2} + \frac{13}{2}\frac{u^2s_2}{st} - \frac{5}{2}\frac{u^3}{ts_2} - \frac{5}{2}\frac{u^3}{st} + 6\frac{ts_2}{s} - 3\frac{ts_2}{u}$$

$$- \frac{21}{4}\frac{tu}{s} - \frac{19}{2}\frac{tu}{s_2} - 2\frac{t^2}{s} + 3\frac{t^2}{u} - 5\frac{t^2}{s_2} - \frac{t^3}{us_2} + 2\frac{ss_2}{t} - 6\frac{ss_2}{u} + 6\frac{su}{t}$$

$$- 24\frac{su}{s_2} - \frac{17}{2}\frac{su^2}{ts_2} + 12\frac{st}{u} - 21\frac{st}{s_2} - 6\frac{st^2}{us_2} + 6\frac{s^2}{t} + 12\frac{s^2}{u} - 24\frac{s^2}{s_2} - 10\frac{s^2u}{ts_2}$$

$$\left. - 12\frac{s^2t}{us_2} - 8\frac{s^3}{us_2} - 4\frac{s^3}{ts_2} \right)$$

$$+ I_4(1, 1, t, 1) \left(-\frac{s_2(s + u)}{2s} - \frac{(s + u)(4s^2 - t^2 + tu + 4u^2 + 2s(t + 4u))}{4st} \right.$$

$$\left. - \frac{4s^3 - u(t + u)^2 + 4s^2(t + 2u) + s(t^2 + 2tu + 3u^2)}{4s(Q^2 + s - s_2)} \right)$$

$$+ \frac{2Q^2(s + Q^2)^2}{s} I_4(1, 2, t, -1) \bigg\} + \bigg\{ t \longleftrightarrow u \bigg\} . \tag{35}$$

Here, $A = s_2^{\mathrm{max}}$ as defined in Eq. (28), $\lambda = \lambda(s, Q^2, s_2)$ with $\lambda(x, y, z) = \sqrt{x^2 + y^2 + z^2 - 2(xy + yz + zx)}$ being Källén's function, we have introduced the short-hand notations

$$L_s = \ln \frac{s}{Q^2}, \quad L_t = \ln \frac{-t}{Q^2}, \quad L_u = \ln \frac{-u}{Q^2}, \quad L_A = \ln \frac{A}{Q^2}, \quad L_{\mu_F} = \ln \frac{\mu_F^2}{Q^2},$$

$$L_{st} = \ln \frac{st^2}{Q^2(s_2 - t)^2}, \quad L_{su} = \ln \frac{su^2}{Q^2(s_2 - u)^2}, \quad L_\lambda = \ln \frac{s + Q^2 - s_2 + \lambda}{s + Q^2 - s_2 - \lambda},$$

$$L_{\lambda t} = \ln \frac{sQ^2(s_2 - t)^2}{[s_2(2Q^2 - u) - Q^2 t]^2}, \quad L_{\lambda u} = \ln \frac{sQ^2(s_2 - u)^2}{[s_2(2Q^2 - t) - Q^2 u]^2}, \tag{36}$$

and we have adopted the following phase-space integrals from Appendix C in Ref. [39]:

$$I_4(1, 1, t, 1) = \frac{1}{\sqrt{X_+}} \ln \frac{u(Q^2 - s_2) + 2Q^2 s + \sqrt{X_+}}{u(Q^2 - s_2) + 2Q^2 s - \sqrt{X_+}},$$

$$I_4(1, 1, t, -1) = \frac{1}{\sqrt{X_-}} \ln \frac{2Q^4 - Q^2(t + u) - st + \sqrt{X_-}}{2Q^4 - Q^2(t + u) - st - \sqrt{X_-}},$$

$$I_4(1, 2, t, -1) = \frac{4Q^6 + st(t + u) - 2Q^4(s + 2(t + u)) + Q^2(-2s^2 - 2s(t + u) + (t + u)^2)}{2Q^2 s X_-}$$

$$+ \frac{2Q^6 - s(s + u)t + Q^2 u(s + t + u) - Q^4(2s + 3u + t)}{2X_-} I_4(1, 1, t, -1) , \tag{37}$$

where

$$X_+ = [u(Q^2 - s_2) + 2Q^2 s]^2 - 4Q^4 s(s + u),$$

$$X_- = [2Q^4 - Q^2(t + u) - st]^2 - 4Q^4 s(s + u). \tag{38}$$

B   Cross section of $q + g \to Z + X$ through $\mathcal{O}(\alpha^2 \alpha_s)$

In this appendix, we consider $\mathcal{O}(\alpha^2 \alpha_s)$ contributions to $q + g \to Z + X$. This includes the virtual QED corrections to subprocess (12) and the real corrections from subprocess (21). We have

$$\frac{s\, d\sigma^{qg}}{dt\, du} = \frac{2\pi \alpha \alpha_s Q_q^2(v_q^2 + a_q^2) C_F}{(N_c^2 - 1)s} \left[\delta(s_2) B_0 + \frac{\alpha}{\pi} \left(\delta(s_2) B_1 + B_2 \right) \right] , \tag{39}$$

18

where

$$B_0 = -\left[\frac{s}{t} + \frac{t}{s} + 2\left(\frac{u}{t} + \frac{u}{s} + \frac{u^2}{st}\right)\right], \tag{40}$$

$$
\begin{aligned}
B_1 &= B_0\left[L_{\mu_F}\left(L_u - L_A - \frac{3}{4}\right) + \frac{1}{2}L_A^2 - \frac{3}{4}L_A\right] \\
&\quad + \frac{(t+u)^2 + u^2}{2st}\left(2\mathrm{Li}_2\left(\frac{Q^2}{s}\right) + L_s^2 + 2L_s L_u - 2L_s \ln\frac{s - Q^2}{Q^2}\right) \\
&\quad - \frac{(s+u)^2 + u^2}{st}\left(\mathrm{Li}_2\left(\frac{t}{Q^2}\right) - L_t L_u + L_t \ln\frac{s+u}{Q^2}\right) \\
&\quad - \frac{(s+u)^2 + (t+u)^2 + 2u^2}{st}\left(\mathrm{Li}_2\left(\frac{u}{Q^2}\right) + L_u \ln\frac{s+t}{Q^2}\right) \\
&\quad + \frac{(s+u)^2 + (t+u)^2}{2st}L_u^2 - \frac{2u(2s + 2t + u)}{(s+t)^2}L_u + \left(-\frac{2u+t}{s+u} + \frac{st}{2(s+u)^2}\right)L_t \\
&\quad - \left(\frac{s+4u}{2(t+u)} + \frac{su}{2(t+u)^2}\right)L_s - \frac{2(2s^2 + 4su + 5u^2)}{st}\zeta(2) - \frac{u}{2(t+u)} \\
&\quad - \frac{2u}{s+t} + \frac{s}{2(s+u)} + \frac{11(s^2 + t^2) - 2st + 20(su + tu) + 18u^2}{4st}, \tag{41}
\end{aligned}
$$

$$
\begin{aligned}
B_2 &= \frac{1}{\lambda}L_\lambda\left[\frac{3s(t-u)^2(t+u)(-2Q^2 + t + u)}{8t\lambda^4}\right. \\
&\quad + \frac{1}{\lambda^2}\left(\frac{(t-u)^2(t+u) - s(t^2 + u^2)}{4t} + \frac{(t-u)(t+u)^2}{8s}\right. \\
&\quad + \left.\frac{Q^2(-t^3 + s^2(3t - u) + tu^2 - 2s(3t^2 - 4tu + u^2))}{4st}\right) \\
&\quad + \frac{64Q^4 + 7s^2 + 7t^2 + 21tu + 16u^2 + 2s(t+u) - 2Q^2(30s + 15t + 16u)}{8st} \\
&\quad \left. - \frac{t^3 + 3t^2u + 4tu^2 + 2u^3}{2st(s_2)_{A+}}\right] + L_{\mu_F}\frac{s^2 + t^2 + 2su + 2tu + 2u^2}{st(s_2)_{A+}} \\
&\quad + L_{su}\left[-\frac{t^2 + 2tu + 2u^2}{2st(s_2)_{A+}} + \frac{1}{2s} - \frac{1}{2t} + \frac{Q^2}{st} + \frac{Q^2(Q^2 - t - s)}{2su^2}\right. \\
&\quad \left. - \frac{1}{u} + \frac{Q^2}{su} - \frac{t}{2su} + \frac{u}{st} - \frac{2Q^4 - 2Q^2(s+t) + (s+t)^2}{2st(Q^2 - u)}\right]
\end{aligned}
$$

19

$$+ \ln \frac{tu - s_2 Q^2}{(s_2 - t)(s_2 - u)} \left[-\frac{s^2 + 2su + 2u^2}{st(s_2)_{A+}} + \left(Q^2 + t - \frac{2Q^2}{st} \left((s-u)^2 + (t-u)^2 \right) \right) \right.$$

$$\left. + \frac{t^2 + (t - 2u)^2}{s} \right) \frac{1}{tu - s_2 Q^2} + \frac{2Q^2(u - s_2) + (s + t)^2}{st(Q^2 - u)} + \frac{-2Q^2 + 3t - 2u}{st} \right]$$

$$+ L_{\lambda t} \left(\frac{2Q^2(u - s_2) + (s + t)^2}{2st(Q^2 - u)} - \frac{s_2 - 2Q^2}{st} \right)$$

$$- \left[\frac{(s + u)^2 + (t + u)^2}{sts_2} \ln \frac{s_2}{Q^2} \right]_{A+} - \ln \frac{\mu_F^2}{s_2} \left(-\frac{st}{(s_2 - t)^3} + \frac{u + t}{(s_2 - t)^2} \right.$$

$$- \frac{3s^2 - 4st + 2t^2 + 6su - 4tu + 4u^2}{2st(s_2 - t)} - \frac{1}{s_2 - u} + \frac{Q^2(u - s_2)}{2u^2 s}$$

$$+ \frac{t((s + t)^2 + su + (t - 4u)^2) - Q^2(2(s^2 + t^2) + st + 4(su - tu + u^2))}{st(tu - s_2 Q^2)}$$

$$+ \frac{5}{2s} - \frac{Q^2}{2t^2} + \frac{3}{2t} - \frac{1}{u} + \frac{Q^2}{su} - \frac{t}{2su} \right)$$

$$+ \frac{3(s^2 + t^2 + 2su + 2tu + 2u^2)}{4st(s_2)_{A+}} + \frac{3s(t - u)^2(t + u)}{4t\lambda^4}$$

$$+ \frac{-2t^3 - 4Q^2(s - 2t)(t - u) + 2tu^2 - 2s^2(t + u) + s(7t^2 - 10tu + 3u^2)}{8st\lambda^2}$$

$$+ \frac{t(s^2 + su + 4(t - u)u) - Q^2(s(t - 4u) + 4u(t - u))}{2st(tu - s_2 Q^2)} + \frac{4st}{(s_2 - t)^3}$$

$$- \frac{4u + 8t - 3s}{2(s_2 - t)^2} + \frac{-s^2 - 4st + 3t^2 + 2su - 2tu + u^2}{2st(s_2 - t)} - \frac{s}{t(s_2 - u)}$$

$$- \frac{3}{2s} - \frac{Q^2}{4t^2} + \frac{3}{8t} - \frac{Q^2(u - s_2)}{2u^2 s} - \frac{1}{u} + \frac{Q^2}{su} - \frac{t}{su} . \tag{42}$$

C Cross section of $q + q \to Z + X$ through $\mathcal{O}(\alpha^2 \alpha_s)$

In this appendix, we consider $\mathcal{O}(\alpha^2 \alpha_s)$ contributions to $q + q \to Z + X$. This includes the interference contributions from subprocess (18) involving a virtual photon or Z boson. We have

$$\frac{s \, d\sigma^{qq}}{dt \, du} = \frac{4\alpha_s \alpha^2 C_F}{N_c s} \left[Q_q^2 (v_q^2 + a_q^2) C_1 + (v_q^4 + 6v_q^2 a_q^2 + a_q^4) C_2 \right] , \tag{43}$$

where

$$C_1 = \frac{s_2^2 + (s - Q^2)^2}{tu} \ln \frac{(s_2 - t)(s_2 - u)}{ss_2} + \frac{2s_2 Q^2(t^2 + u^2) - tu(t + u)^2}{t^2 u^2}$$

$$+ s \left\{ \frac{s^2 + (s_2 - Q^2)^2}{2(s + Q^2 - s_2)(s_2 - t)t} L_{\lambda t} + \left(\frac{s^2 + (s_2 - Q^2)^2}{2(s + Q^2 - s_2)(s_2 - t)t} \right. \right.$$

$$+ \frac{2suQ^2 + t(2s_2(s - Q^2) + (t+u)^2)}{2sut^2}\Bigg) L_{st}\Bigg\} + s\Big\{ u \leftrightarrow t \Big\}, \tag{44}$$

$$C_2 = \frac{s(2s_2 Q^2(t^2 + u^2) - tu(t+u)^2)}{t^2 u^2(s+Q^2)} + \Bigg\{ -\frac{1}{4(Q^2+s)^2 tu} \ln \frac{(Q^2 t - s_2(s+Q^2))^2}{Q^2(s+t)(s_2-t)^2}$$

$$\left(Q^2(s_2^2 + (s_2 - t)^2 - u(2s+u)) + s(2s_2(s-Q^2) + (t+u)^2) \right)$$

$$+ L_{st}\Bigg[\frac{-s^2}{2(Q^2+s)^2 t} + \frac{s^2}{2(Q^2 + s - s_2)t(s+u)} - \frac{s+t}{4t(s+u)} - \frac{1}{4t}$$

$$+ \frac{t^2 - u^2 + 2s_2^2 - 2s_2 t}{4(Q^2+s)tu} + \frac{s_2 Q^2}{2t^2(s+u)}\Bigg] + \frac{s^2 + (Q^2 - s_2)^2}{4(Q^2 + s - s_2)t(s+u)} L_{\lambda t}$$

$$+ \frac{Q^2(s_2 - u)}{2u^2(s+t)} \ln \frac{Q^2}{s+t} + \frac{1}{4} I_4(1,1,t,1)\Bigg[\frac{s^2(Q^2 - s - s_2)}{(Q^2 + s - s_2)(s+u)}$$

$$+ \frac{(2s_2^2 + t(Q^2 - s_2))s}{t(s+u)} - \frac{(-2s_2 + t + u)^2}{t}\Bigg]$$

$$+ I_4(1,1,t,-1)\Bigg[-\frac{s^3}{2(Q^2 + s - s_2)(s+u)} - \frac{s^2 Q^2}{2(Q^2+s)^2} + \frac{s(Q^2 - u)}{Q^2 + s}$$

$$+ \frac{s_2 s(u - Q^2)}{2(Q^2+s)u} - \frac{s(u-t)^2}{4t(Q^2+s)} + \frac{s_2 s(u - s_2)}{2(Q^2+s)t} + \frac{s^2(2t - s_2)}{4t(s+u)}$$

$$- \frac{5s_2 t}{4(s+u)} + \frac{s_2^2(2t - s_2)}{t(s+u)} + \frac{t^2}{4(s+u)} + \frac{s(2s_2 - t)}{4(s+u)} + \frac{u^2}{2t} - \frac{5s_2}{2} + \frac{t}{2} + u$$

$$- \frac{9s_2 u}{4t} + \frac{3s_2^2}{t} - \frac{s_2^2}{u} - \frac{t^2}{4u} + \frac{s_2 t}{u} - \frac{5s_2 s}{4t} + \frac{s_2 s}{2u}\Bigg] - \frac{Q^2 s^2}{Q^2 + s} I_4(1,2,t,-1)\Bigg\} + \Big\{ t \leftrightarrow u \Big\}. \tag{45}$$

Here, we have again used the phase-space integrals given in Eq. (37).

References

[1] G. Arnison *et al.* (UA1 Collaboration), Phys. Lett. **122B** (1983) 103; M. Banner *et al.* (UA2 Collaboration), Phys. Lett. **122B** (1983) 476.

[2] G. Arnison *et al.* (UA1 Collaboration), Phys. Lett. **126B** (1983) 398; P. Bagnaia *et al.* (UA2 Collaboration), Phys. Lett. **129B** (1983) 130.

[3] G. Altarelli, R. K. Ellis and G. Martinelli, Nucl. Phys. B **143** (1978) 521 [Erratum-ibid. B **146** (1978) 544]; Nucl. Phys. B **157** (1979) 461; J. Kubar-André and F. E. Paige, Phys. Rev. D **19** (1979) 221; J. Abad, B. Humpert and W. L. van Neerven, Phys. Lett. B **83** (1979) 371; K. Harada, T. Kaneko and N. Sakai, Nucl.

Phys. B **155** (1979) 169 [Erratum-ibid. B **165** (1980) 545]; P. Aurenche and J. Lindfors, Nucl. Phys. B **185** (1981) 274.

[4] T. Matsuura, S. C. van der Marck and W. L. van Neerven, Nucl. Phys. B **319** (1989) 570; R. Hamberg, W. L. van Neerven and T. Matsuura, Nucl. Phys. B **359** (1991) 343 [Erratum-ibid. B **644** (2002) 403]; W. L. van Neerven and E. B. Zijlstra, Nucl. Phys. B **382** (1992) 11 [Erratum-ibid. B **680** (2004) 513]; P. J. Rijken and W. L. van Neerven, Phys. Rev. D **51** (1995) 44 [arXiv:hep-ph/9408366]; R. V. Harlander and W. B. Kilgore, Phys. Rev. Lett. **88** (2002) 201801 [arXiv:hep-ph/0201206]; C. Anastasiou, L. J. Dixon, K. Melnikov and F. Petriello, Phys. Rev. Lett. **91** (2003) 182002 [arXiv:hep-ph/0306192]; Phys. Rev. D **69** (2004) 094008 [hep-ph/0312266]; V. Ravindran, J. Smith and W. L. van Neerven, Nucl. Phys. B **682** (2004) 421 [arXiv:hep-ph/0311304]; K. Melnikov and F. Petriello, Phys. Rev. Lett. **96** (2006) 231803 [hep-ph/0603182]; Phys. Rev. D **74** (2006) 114017 [hep-ph/0609070]; S. Catani, L. Cieri, G. Ferrera, D. de Florian and M. Grazzini, Phys. Rev. Lett. **103** (2009) 082001 [arXiv:0903.2120 [hep-ph]].

[5] S. Moch and A. Vogt, Phys. Lett. B **631** (2005) 48 [hep-ph/0508265]; E. Laenen and L. Magnea, Phys. Lett. B **632** (2006) 270 [hep-ph/0508284]; A. Idilbi, X. Ji, J.-P. Ma and F. Yuan, Phys. Rev. D **73** (2006) 077501 [hep-ph/0509294]; V. Ravindran and J. Smith, Phys. Rev. D **76** (2007) 114004 [arXiv:0708.1689 [hep-ph]]; N. Kidonakis, Phys. Rev. D **77** (2008) 053008 [arXiv:0711.0142 [hep-ph]]; S. Marzani and R. D. Ball, Nucl. Phys. B **814** (2009) 246 [arXiv:0812.3602 [hep-ph]].

[6] U. Baur, S. Keller and D. Wackeroth, Phys. Rev. D **59** (1999) 013002 [arXiv:hep-ph/9807417]; V. A. Zykunov, Eur. Phys. J. direct C **3** (2001) 9 [arXiv:hep-ph/0107059]; Yad. Fiz. **66** (2003) 910 [Phys. Atom. Nucl. **66** (2003) 878]; S. Dittmaier and M. Krämer, Phys. Rev. D **65** (2002) 073007 [arXiv:hep-ph/0109062]; U. Baur and D. Wackeroth, Phys. Rev. D **70** (2004) 073015 [hep-ph/0405191]; A. Arbuzov, D. Bardin, S. Bondarenko, P. Christova, L. Kalinovskaya, G. Nanava and R. Sadykov, Eur. Phys. J. C **46** (2006) 407 [Erratum-ibid. C **50** (2007) 505] [hep-ph/0506110]; C. M. Carloni Calame, G. Montagna, O. Nicrosini and A. Vicini, JHEP **0612** (2006) 016 [hep-ph/0609170]; S. Brensing, S. Dittmaier, M. Krämer and A. Mück, Phys. Rev. D **77** (2008) 073006 [arXiv:0710.3309 [hep-ph]].

[7] U. Baur, S. Keller and W. K. Sakumoto, Phys. Rev. D **57** (1998) 199 [hep-ph/9707301]; U. Baur, O. Brein, W. Hollik, C. Schappacher and D. Wackeroth, Phys. Rev. D **65** (2002) 033007 [arXiv:hep-ph/0108274]; V. A. Zykunov, Yad. Fiz. **69** (2006) 1557 [Phys. Atom. Nucl. **69** (2006) 1522]; Phys. Rev. D **75** (2007) 073019 [arXiv:hep-ph/0509315]; Yad. Fiz. **71** (2008) 757 [Phys. Atom. Nucl. **71** (2008) 732]; C. M. Carloni Calame, G. Montagna, O. Nicrosini and A. Vicini, JHEP **0710** (2007) 109 [arXiv:0710.1722 [hep-ph]]; A. Arbuzov, D. Bardin, S. Bondarenko, P. Christova, L. Kalinovskaya, G. Nanava and R. Sadykov, Eur. Phys. J. C **54** (2008) 451 [arXiv:0711.0625 [hep-ph]]; S. Dittmaier and M. Huber, JHEP **1001** (2010) 060 [arXiv:0911.2329 [hep-ph]].

[8] A. Kotikov, J. H. Kühn and O. Veretin, Nucl. Phys. B **788** (2008) 47 [hep-ph/0703013 [HEP-PH]].

[9] J. Fleischer, A. V. Kotikov and O. L. Veretin, Nucl. Phys. B **547** (1999) 343 [arXiv:hep-ph/9808242].

[10] S. Dittmaier, A. Huss and C. Schwinn, Nucl. Phys. B **885** (2014) 318 [arXiv:1403.3216 [hep-ph]].

[11] R. K. Ellis, G. Martinelli and R. Petronzio, Nucl. Phys. B **211** (1983) 106; J. J. van der Bij and E. W. N. Glover, Nucl. Phys. B **313** (1989) 237; P. B. Arnold and M. H. Reno, Nucl. Phys. B **319** (1989) 37 [Erratum-ibid. B **330** (1990) 284]; F. T. Brandt, G. Kramer and S.-L. Nyeo, Z. Phys. C **48** (1990) 301; Int. J. Mod. Phys. A **6** (1991) 3973; W. T. Giele, E. W. N. Glover and D. A. Kosower, Nucl. Phys. B **403** (1993) 633 [arXiv:hep-ph/9302225]; L. J. Dixon, Z. Kunszt and A. Signer, Nucl. Phys. B **531** (1998) 3 [hep-ph/9803250]; J. M. Campbell and R. K. Ellis, Phys. Rev. D **65** (2002) 113007 [arXiv:hep-ph/0202176]; J. M. Campbell, R. K. Ellis and D. L. Rainwater, Phys. Rev. D **68** (2003) 094021 [arXiv:hep-ph/0308195].

[12] R. J. Gonsalves, J. Pawłowski and C. F. Wai, Phys. Rev. D **40** (1989) 2245.

[13] R. J. Gonsalves, N. Kidonakis and A. Sabio Vera, Phys. Rev. Lett. **95** (2005) 222001 [hep-ph/0507317]; K. Melnikov and F. Petriello, Phys. Rev. D **74** (2006) 114017 [arXiv:hep-ph/0609070]. N. Kidonakis and R. J. Gonsalves, Phys. Rev. D **87** (2013) 014001 [arXiv:1201.5265 [hep-ph]]; Phys. Rev. D **89** (2014) 094022 [arXiv:1404.4302 [hep-ph]]; R. Boughezal, C. Focke, X. Liu and F. Petriello, Phys. Rev. Lett. **115** (2015) 6, 062002 [arXiv:1504.02131 [hep-ph]].

[14] J. H. Kühn, A. Kulesza, S. Pozzorini and M. Schulze, Phys. Lett. B **651** (2007) 160 [arXiv:hep-ph/0703283]; Nucl. Phys. B **797** (2008) 27 [arXiv:0708.0476 [hep-ph]].

[15] W. Hollik, T. Kasprzik and B. A. Kniehl, Nucl. Phys. B **790** (2008) 138 [arXiv:0707.2553 [hep-ph]].

[16] J. H. Kühn, A. Kulesza, S. Pozzorini and M. Schulze, Phys. Lett. B **609** (2005) 277 [arXiv:hep-ph/0408308].

[17] J. H. Kühn, A. Kulesza, S. Pozzorini and M. Schulze, Nucl. Phys. B **727** (2005) 368 [arXiv:hep-ph/0507178].

[18] E. W. N. Glover and A. G. Morgan, Z. Phys. C **62** (1994) 311; E. W. N. Glover and A. G. Morgan, Phys. Lett. B **334** (1994) 208.

[19] S. Frixione, Phys. Lett. B **429** (1998) 369 [hep-ph/9801442].

[20] A. Denner, S. Dittmaier, T. Kasprzik and A. Mück, JHEP **0908** (2009) 075 [arXiv:0906.1656 [hep-ph]].

[21] A. Denner, S. Dittmaier, T. Kasprzik and A. Mück, JHEP **1106** (2011) 069 [arXiv:1103.0914 [hep-ph]].

[22] A. Denner, S. Dittmaier, T. Kasprzik and A. Mück, Eur. Phys. J. C **73** (2013) 2297 [arXiv:1211.5078 [hep-ph]].

[23] A. Denner, L. Hofer, A. Scharf and S. Uccirati, JHEP **1501** (2015) 094 [arXiv:1411.0916 [hep-ph]].

[24] S. Kallweit, J. M. Lindert, P. Maierhöfer, S. Pozzorini and M. Schönherr, JHEP **1504** (2015) 012 [arXiv:1412.5157 [hep-ph]].

[25] G. Altarelli and G. Parisi, Nucl. Phys. B **126** (1977) 298.

[26] K.-P. O. Diener, S. Dittmaier and W. Hollik, Phys. Rev. D **72** (2005) 093002 [hep-ph/0509084].

[27] R. K. Ellis and G. Zanderighi, JHEP **0802** (2008) 002 [arXiv:0712.1851 [hep-ph]].

[28] R. W. Brown, L. B. Gordon, J. Smith and K. O. Mikaelian, Phys. Rev. D **13** (1976) 1856; M. Hayashi and K. Katsuura, Prog. Theor. Phys. **61** (1979) 1166.

[29] B. A. Kniehl, Phys. Lett. B **254** (1991) 267.

[30] M. Glück, M. Stratmann and W. Vogelsang, Phys. Lett. B **343** (1995) 399.

[31] A. D. Martin, R. G. Roberts, W. J. Stirling and R. S. Thorne, Eur. Phys. J. C **39** (2005) 155 [hep-ph/0411040].

[32] R. D. Ball *et al.* (NNPDF Collaboration), Nucl. Phys. B **877** (2013) 290 [arXiv:1308.0598 [hep-ph]].

[33] M. Tentyukov and J. Fleischer, Comput. Phys. Commun. **132** (2000) 124 [hep-ph/9904258].

[34] T. Hahn, Comput. Phys. Commun. **140** (2001) 418 [hep-ph/0012260].

[35] J. Kuipers, T. Ueda, J. A. M. Vermaseren and J. Vollinga, Comput. Phys. Commun. **184** (2013) 1453 [arXiv:1203.6543 [cs.SC]].

[36] J. Beringer *et al.* (Particle Data Group), Phys. Rev. D **86** (2012) 010001.

[37] S. Frixione, V. Hirschi, D. Pagani, H.-S. Shao and M. Zaro, JHEP **1506** (2015) 184 [arXiv:1504.03446 [hep-ph]].

[38] P. Aurenche, M. Fontannaz and J. Ph. Guillet, Eur. Phys. J. C **44** (2005) 395 [hep-ph/0503259].

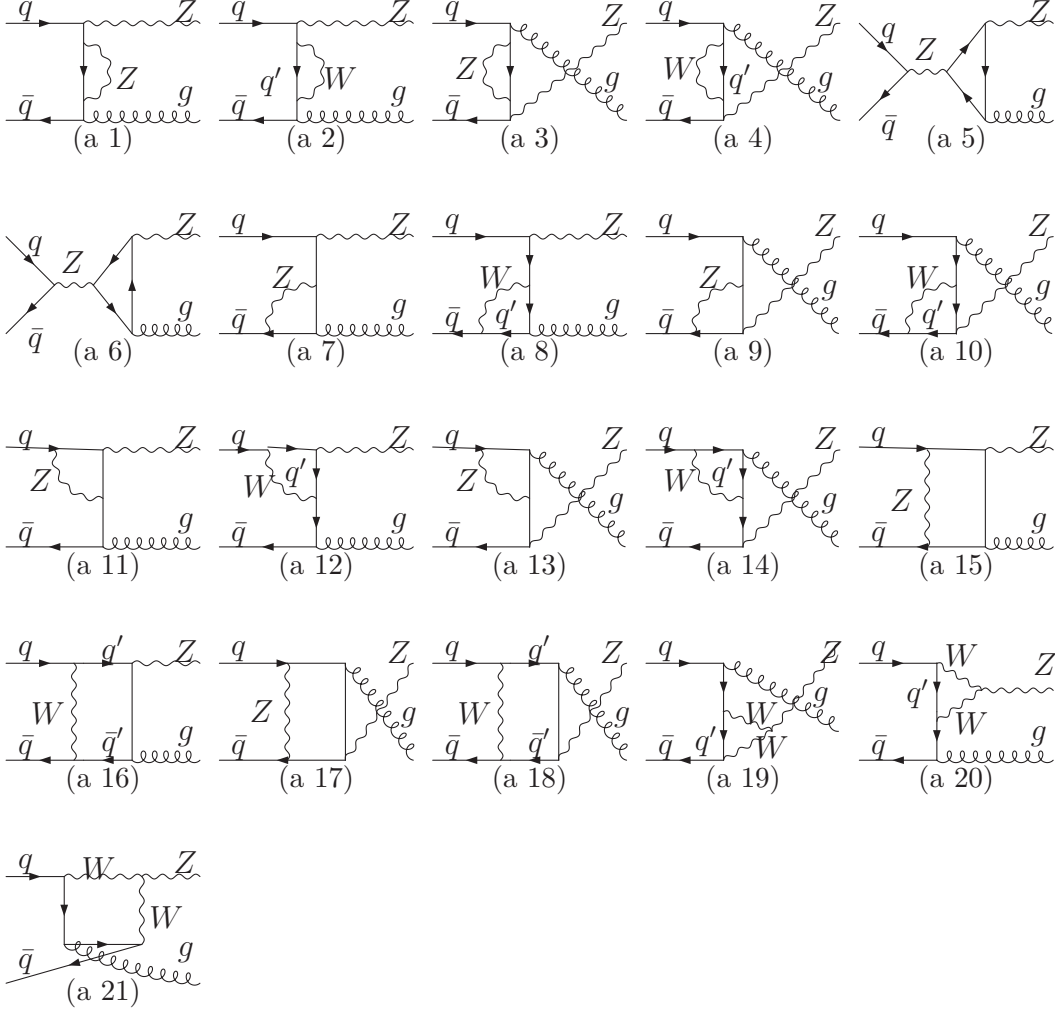[39] W. Beenakker, H. Kuijf, W. L. van Neerven and J. Smith, Phys. Rev. D **40** (1989) 54.

Figure 3: Weak-interaction one-loop diagrams contributing to the partonic subprocess $q + \bar{q} \rightarrow Z + g$ at $\mathcal{O}(\alpha^2 \alpha_s)$. The weak-interaction one-loop diagrams contributing to the partonic subprocess $q + g \rightarrow Z + q$ at $\mathcal{O}(\alpha^2 \alpha_s)$ are obtained by appropriately crossing external legs.
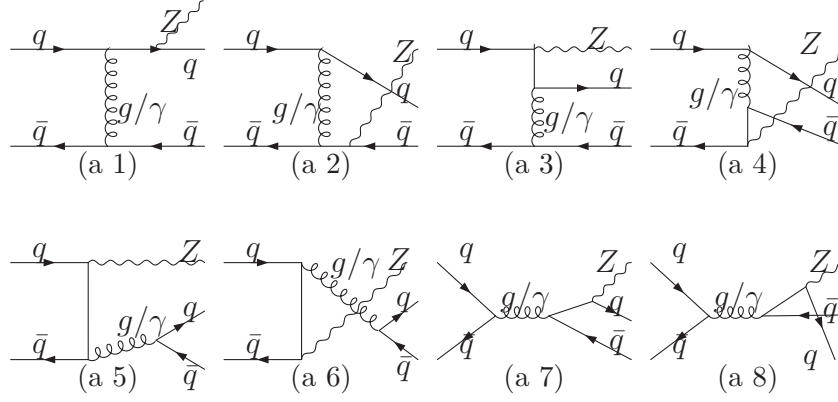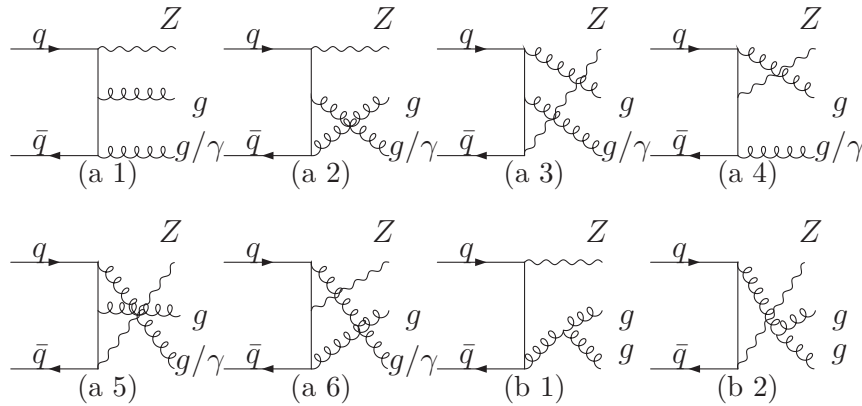
Figure 4: Tree-level diagrams contributing to the partonic subprocess $q + \bar{q} \to Z + q + \bar{q}$ at $\mathcal{O}(\alpha\alpha_s^2)$ (with a virtual gluon). Interferences of diagrams (a 5)–(a 8) with a virtual photon or Z boson (gluon) with diagrams (a 1)–(a 4) with a virtual gluon (photon or Z boson) contribute at $\mathcal{O}(\alpha^2\alpha_s)$.

Figure 5: Tree-level diagrams contributing to the partonic subprocess $q + \bar{q} \to Z + g + g$ at $\mathcal{O}(\alpha\alpha_s^2)$ and to the partonic subprocess $q + \bar{q} \to Z + g + \gamma$ at $\mathcal{O}(\alpha^2\alpha_s)$.
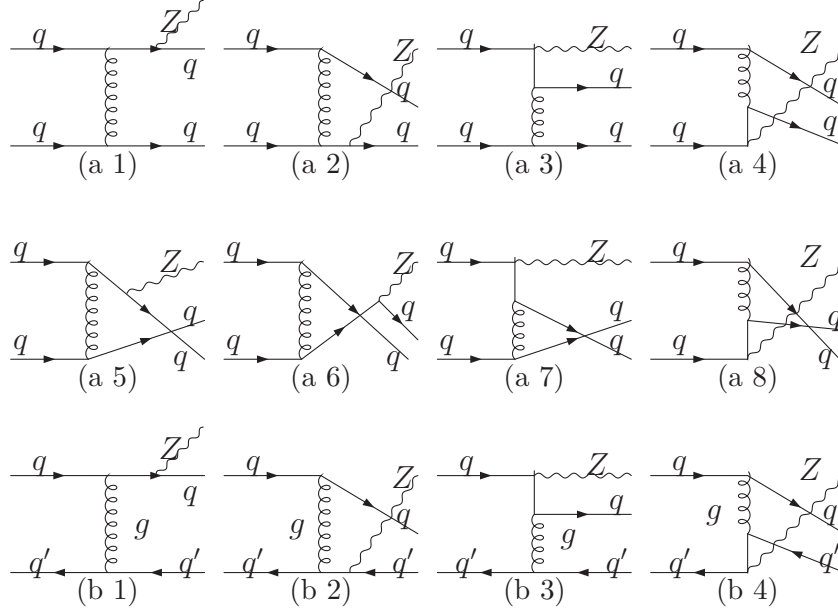
Figure 6: Tree-level diagrams contributing to the partonic subprocesses $q + q \to Z + q + q$ and $q + q' \to Z + q + q'$ at $\mathcal{O}(\alpha \alpha_s^2)$. Interferences of diagrams (a 5)–(a 8) with the gluon replaced by a photon or Z boson with diagrams (a 1)–(a 4) contribute at $\mathcal{O}(\alpha^2 \alpha_s)$.
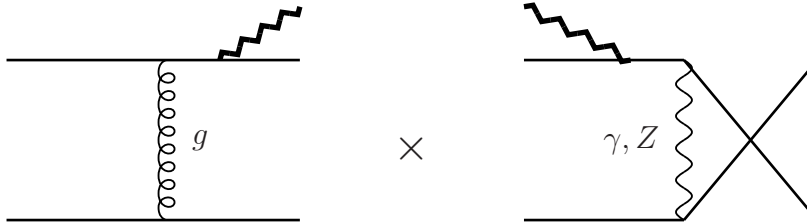
Figure 7: $\mathcal{O}(\alpha^{1/2} \alpha_s)$ and $\mathcal{O}(\alpha^{3/2})$ tree-level diagrams interfering to yield $\mathcal{O}(\alpha^2 \alpha_s)$ contributions to subprocesses $q + \bar{q} \to Z + q + \bar{q}$ and $q + q \to Z + q + q$.
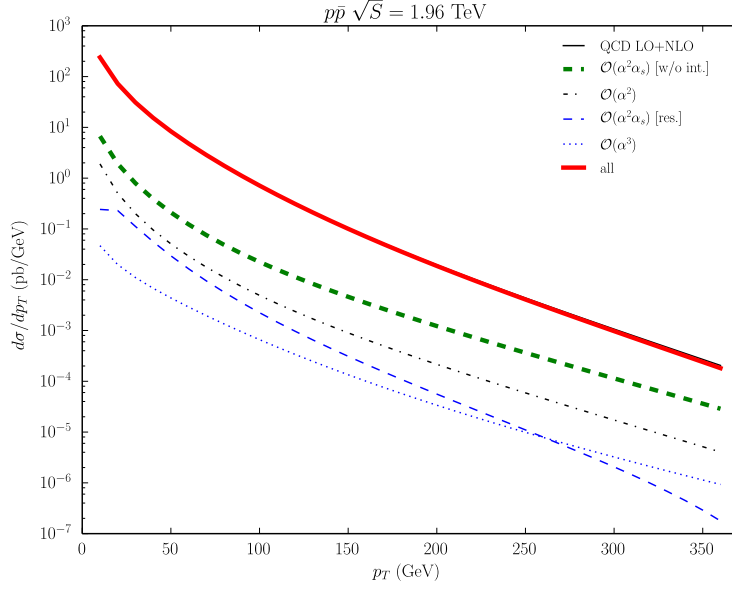
(a)
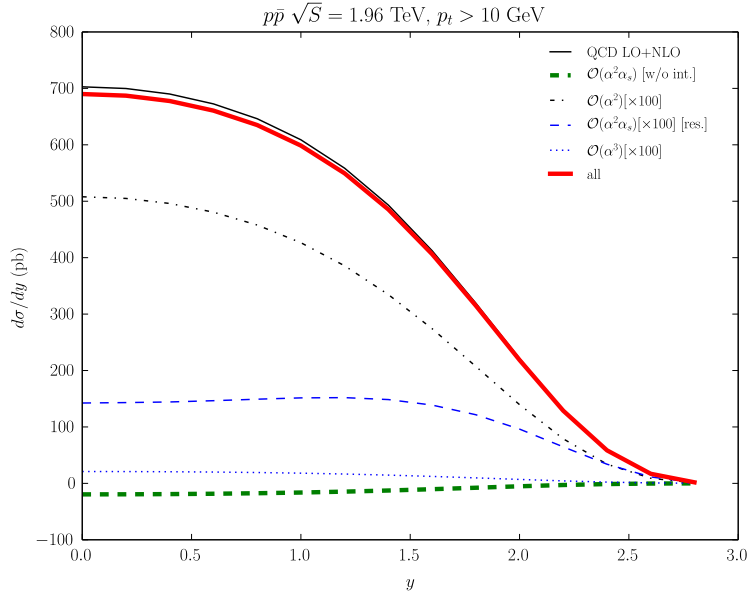
(b)

Figure 8: Cross section distributions in (a) p_T and (b) y for $p_T > 10$ GeV of $p\bar{p} \to Z + X$ at $\sqrt{S} = 1.96$ TeV (Tevatron run II). In each frame, the NLO QCD result [12], i.e. the sum of the $\mathcal{O}(\alpha\alpha_s)$ and $\mathcal{O}(\alpha\alpha_s^2)$ results (thin solid lines), the $\mathcal{O}(\alpha^2)$ Born result (thin dot-dashed lines), the purely weak $\mathcal{O}(\alpha^2\alpha_s)$ corrections to subprocesses (10) and (12) [17] (thick dashed green lines), the residual electroweak $\mathcal{O}(\alpha^2\alpha_s)$ corrections (thin dashed blue lines), the $\mathcal{O}(\alpha^3)$ photoproduction contributions (thin dotted blue lines), and the total sum (thick solid red lines) are shown.
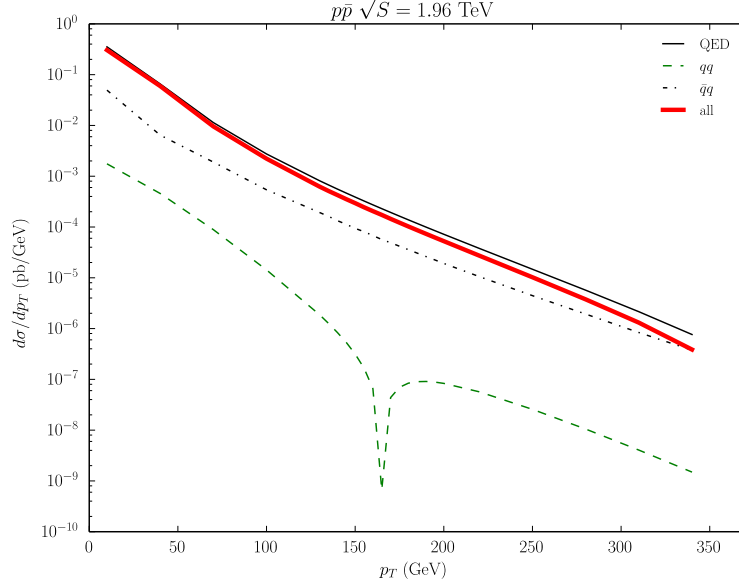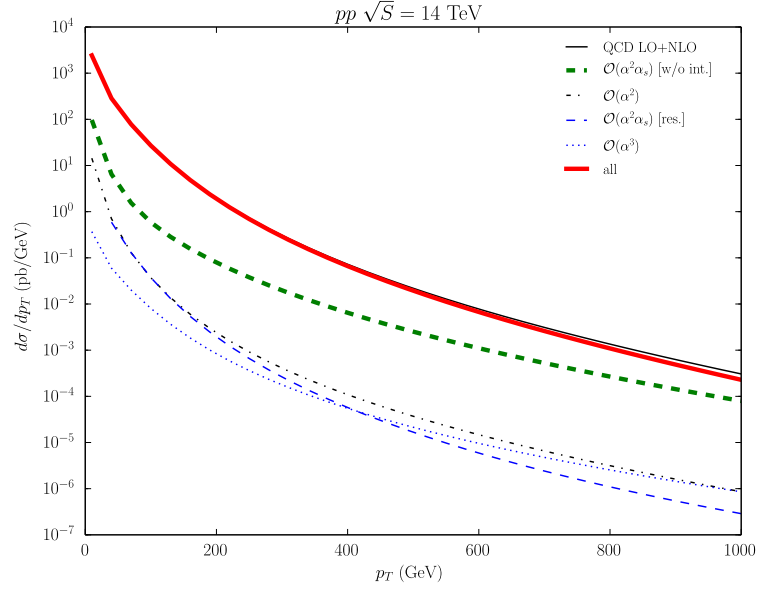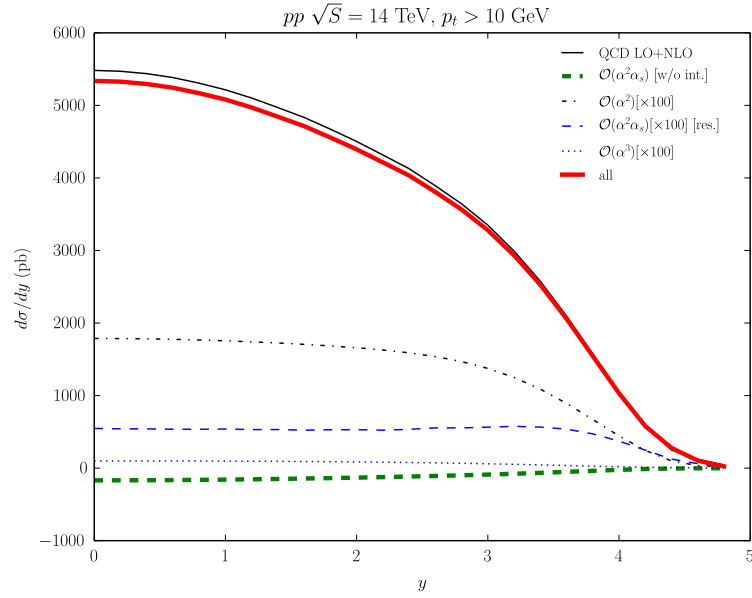
(a)
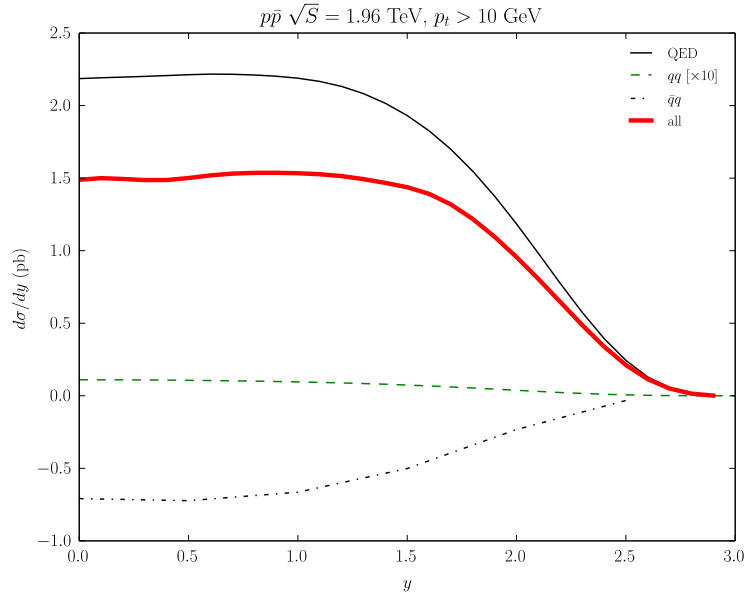
(b)

Figure 9: The residual electroweak $\mathcal{O}(\alpha^2\alpha_s)$ corrections in Fig. 8 (thick solid red lines) are decomposed into the combination of the $\mathcal{O}(\alpha)$ QED corrections to subprocesses (10) and (12) and the $\mathcal{O}(\alpha_s)$ QCD corrections to subprocess (11) (thin solid lines), and the QCD-electroweak interference contributions from subprocesses (14) (thin dot-dashed lines) and (18) (thin dashed green lines).
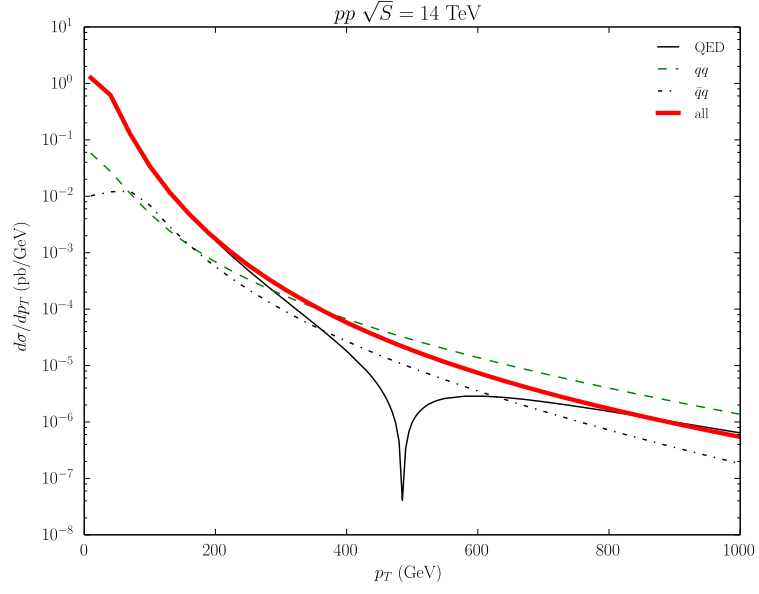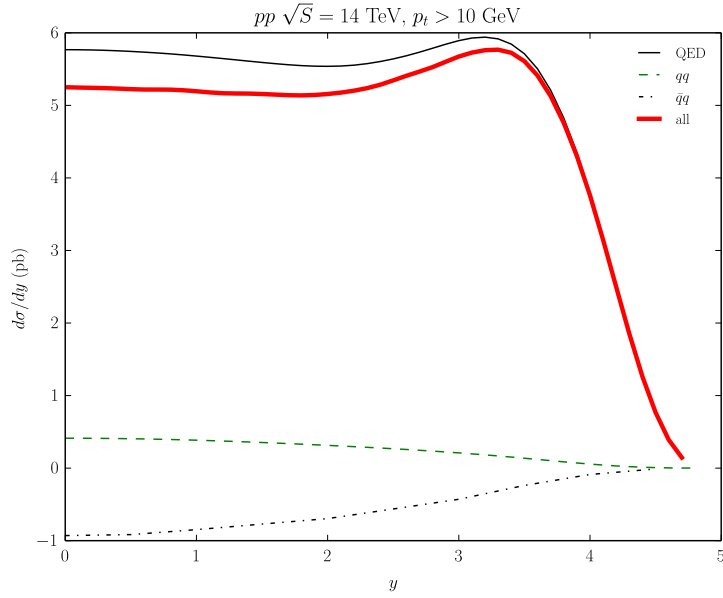
(a)

(b)

Figure 10: Same as in Fig. 8, but for $pp \to Z + X$ at $\sqrt{S} = 14$ TeV (LHC).

(a)

(b)

Figure 11: Same as in Fig. 9, but for $pp \rightarrow Z + X$ at $\sqrt{S} = 14$ TeV (LHC).